

# Accelerating Diffusion Sampling via Exploiting Local Transition Coherence

Shangwen Zhu\*, Han Zhang\*, Zhantao Yang\*, Qianyu Peng, Zhao Pu  
Huangji Wang, Fan Cheng†  
Shanghai Jiao Tong University, Shanghai, China

## Abstract

Text-based diffusion models have made significant breakthroughs in generating high-quality images and videos from textual descriptions. However, the lengthy sampling time of the denoising process remains a significant bottleneck in practical applications. Previous methods either ignore the statistical relationships between adjacent steps or rely on attention or feature similarity between them, which often only works with specific network structures. To address this issue, we discover a new statistical relationship in the transition operator between adjacent steps, focusing on the relationship of the outputs from the network. This relationship does not impose any requirements on the network structure. Based on this observation, we propose a novel **training-free** acceleration method called **LTC-ACCEL**, which uses the identified relationship to estimate the current transition operator based on adjacent steps. Due to no specific assumptions regarding the network structure, **LTC-ACCEL** is applicable to almost all diffusion-based methods and orthogonal to almost all existing acceleration techniques, making it easy to combine with them. Experimental results demonstrate that **LTC-ACCEL** significantly speeds up sampling in text-to-image and text-to-video synthesis while maintaining competitive sample quality. Specifically, **LTC-ACCEL** achieves a speedup of **1.67×** in **Stable Diffusion v2** and a speedup of **1.55×** in video generation models. When combined with distillation models, **LTC-ACCEL** achieves a remarkable **10×** speedup in video generation, allowing **real-time** generation of more than **16FPS**. Our code is available on [Project Page](#).

## 1. Introduction

Recent advancements in text-based generation, particularly with diffusion models [6, 9, 27, 29, 30], have significantly improved the generation of high-fidelity images [1, 7, 19, 43, 49, 57], audio [14, 17, 18, 24, 34, 45, 46],

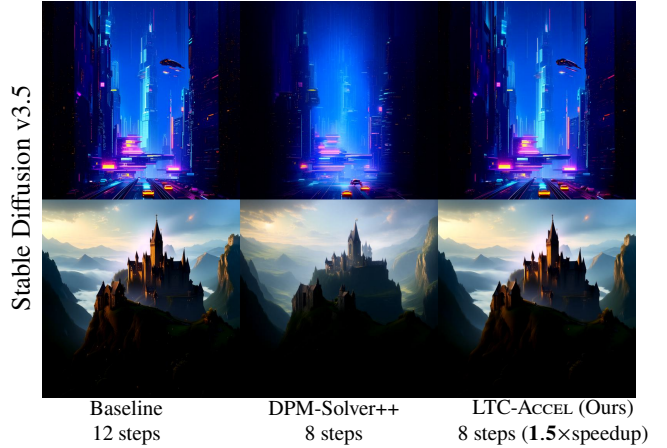


**Figure 1.** Comparison between LTC-ACCEL with DPM-Solver++ when implemented on Stable Diffusion v3.5 under the same number of steps and speedup framework. Results show that LTC-ACCEL significantly outperforms DPM-Solver++.

and video [4, 11, 16, 20, 28, 31, 52, 53] from textual descriptions, achieving remarkable advancements in visual fidelity and semantic alignment. By iteratively refining a noisy input until it converges to a sample that aligns with the given text prompt, these models capture intricate details and complex compositions previously unattainable with other approaches. Despite their impressive capabilities, a major drawback of diffusion models, particularly in video generation, is their high computational complexity during the denoising process, leading to prolonged inference times and substantial computational costs. For instance, generating a 5-second video at 8 frames per second (FPS) with a resolution of 720P using Wan2.1-14B [44] on a single H20 GPU takes approximately **6935** seconds, highlighting the significant resource demands of high-quality video synthesis. This limitation poses a considerable challenge for real-time applications and resource-constrained environments [1, 41].

To accelerate diffusion models, various approaches have been proposed, including training-based and training-free strategies. Training-based methods enhance sampling efficiency by modifying the training process [12, 25, 38, 40, 42, 54, 59] or altering model architectures [15, 33, 39, 55], but

\*These authors contributed equally to this work.

†Corresponding author



**Figure 2.** Qualitative results of LTC-ACCEL integrated with existing training-free and training-based methods. Fig. 2a: Integration of LTC-ACCEL with caching-based methods using DDIM on Stable Diffusion v2. Fig. 2b: Integration of LTC-ACCEL with Anime-diff-lightning(distilled version of Anime-diff). Results show that LTC-ACCEL can be combined with previous methods well and achieve additional speedup without compromise on the quality of the generated images.

they require additional computation and extended training. In contrast, training-free methods improve sampling efficiency without modifying the trained model by optimizing the denoising process [5, 10, 32, 37, 51] or introducing more efficient solvers [22, 23, 58]. Additionally, caching-based methods such as DeepCache [26, 47] exploit temporal redundancy in denoising steps to store and reuse intermediate features, thus achieving the reduction of redundant computations. However, these methods require a redesign of the caching strategy when the network architecture changes. Unlike previous methods that rely on attention mechanisms or feature similarity within the network, we identify the phenomenon of **Local Transition Coherence**, which refers to the strong correlation between the transition operators ( $\Delta x_{t+1,t}$ ) of neighboring steps. Based on this insight, we propose LTC-ACCEL, a novel training-free acceleration method that approximates the current step’s transition operator using those from adjacent steps. As a result, it does not depend on any specific network architecture, making it broadly applicable to various diffusion models and compatible with both training-based and training-free acceleration methods.

We conducted extensive experiments demonstrating the effectiveness of our method and its compatibility with other approaches. LTC-ACCEL achieves a **1.67x** speedup on Stable Diffusion v2 [35], and when combined with DeepCache [26], accelerates the process to **2.34x**. It also integrates with Align Your Steps [37], achieving the equivalent of 10 steps of Align Your Steps in just 8 steps on Stable Diffusion v1.5 [35], with minimal impact on generation quality. Additionally, we achieve a **1.67x** speedup on the Anime-Diff model [4], and by combining it with the distilled version,

Anime-Diff-Lightning [20], we achieve a **10x** speedup in video generation, enabling **three-step** generation.

The core contributions of our work are:

- We have identified the phenomenon of Local Transition Coherence. Unlike previous approaches that rely on attention mechanisms or feature similarity within the network, this phenomenon reveals the inherent consistency of update trajectories, which is a broader consistency independent of any specific network architecture and pervasive throughout the diffusion sampling process.
- We propose LTC-ACCEL, a training-free, highly generalizable method applicable to various diffusion models and orthogonal to both training-based and training-free acceleration methods, providing significant acceleration without sacrificing performance.
- We conducted extensive experiments to validate the effectiveness of our method and its compatibility with other approaches. LTC-ACCEL significantly accelerates the generation process of models including Stable Diffusion, CogVideoX and Anime-Diff, and enhances performance when combined with existing acceleration methods.

## 2. Related Work

### 2.1. Training-Based Acceleration Methods

Traditional acceleration methods for diffusion models typically modify the model architecture or the sampling process during training for faster inference speed. Several typical approaches include mixed precision training and lightweight architectures [39, 55]. Recently, distillation [12, 25, 38, 40, 42, 54, 59] has gained popularity, focus-

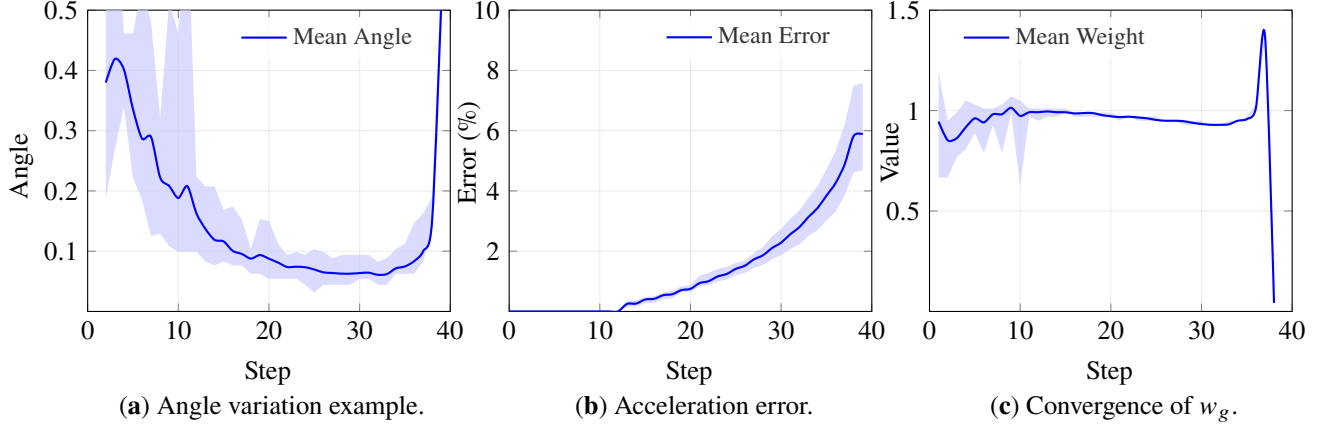


**Figure 3.** Variation of angle, error, and across sampling steps on Stable Diffusion v2 using DDIM with 20 steps and 20 unique prompt-latent pairs. Fig. 3a Angle variation per step. Fig. 3b Error between LTC-ACCEL and the original process, with acceleration ( $r = 2$ ) applied over [12, 38], quantified by the 2-norm difference in latents. Fig. 3c  $w_g$  variation, showing initial oscillations followed by **rapid convergence**.

ing on reducing inference steps without significant quality loss. However, these methods require additional training, which can be both time-consuming and resource-intensive.

## 2.2. Training-Free Acceleration Methods

In certain scenarios where training resources are limited, training-free acceleration methods [5, 10, 32, 51] can outperform the training-based ones since they don’t require any additional training, but are still capable of acceleration with little compromise to the performance. Thus, many successful training-free methods have been proposed and achieved promising effects. Optimized from the DDPM formulation, DDIM [41] is one of the typical attempts that has reduced the number of inference steps by introducing non-Markov process. The DPM-Solver [22, 23, 58] has also achieved significant reduction in the number of inference steps, while the implementation is focused on applying the specific high-order solver to solve diffusion ODEs [8, 56, 60] equivalent to the denoising process. Besides, more recent approaches pay attention to preserving and reusing features from earlier steps, significantly reducing the computational load for subsequent steps. For example, DeepCache [26, 47] has performed exceptionally by reusing cacheable high-level features from consecutive steps and only updating low-level features, thus achieving nearly lossless acceleration. Moreover, optimizations on the sampling schedules have proved to be effective as well. Align Your Steps [37] has broadened its application scenarios by leveraging methods from stochastic calculus and applying optimal schedules specific to various solvers, pre-trained models and datasets.

## 3. LTC-ACCEL for Faster Diffusion Sampling

In this section, we first introduce the newly observed phenomenon called Local Transition Coherence in Sec. 3.1,

which reveals the statistical correlation between the outputs of adjacent transition operations in the diffusion process. Next, in Sec. 3.2, we introduce our method, LTC-ACCEL, which takes advantage of the transition operators of neighboring steps to approximate and replace the transition operator of the current step. Finally, in Sec. 3.3, we analyze the errors introduced by LTC-ACCEL, which is negligible.

### 3.1. Local Transition Coherence

In this section, we introduce the newly observed phenomenon called **Local Transition Coherence**: During certain phases of the diffusion process, the transition operators of consecutive steps exhibit significant similarity. To quantify the difference between steps  $t$  and  $t + 1$ , we define the transition operator as  $\Delta \mathbf{x}_{t+1,t} = \mathbf{x}_t - \mathbf{x}_{t+1}$ . Additionally, we define the angle between the transition operators at successive steps as follows:

**Definition 3.1.** The angle  $\theta$  between  $\Delta \mathbf{x}_{t+1,t}$  and  $\Delta \mathbf{x}_{t+2,t+1}$  is defined as

$$\theta = \arccos \left( \frac{\Delta \mathbf{x}_{t+1,t} \cdot \Delta \mathbf{x}_{t+2,t+1}}{\|\Delta \mathbf{x}_{t+1,t}\|^2 \|\Delta \mathbf{x}_{t+2,t+1}\|^2} \right). \quad (1)$$

Note that when the angle  $\theta$  approaches 0, the update trajectories of the two transition operators are nearly identical, and can be replaced by each other. As shown in Fig. 3a, we observe that the angles are relatively small from steps 12 to 38, suggesting the update trajectories are highly similar during this period. This allows us to reduce unnecessary computations by approximating the current transition operator with that of the adjacent steps, thereby speeding up the sampling process significantly and effectively.

In practice, we define a threshold  $\tau$  to identify the interval where  $\theta$  remains relatively small, referred to as the acceleration interval and formally defined as follows:



**Definition 3.2.** The acceleration interval is defined as the range  $[a, b]$ , where  $a \geq 1$ ,  $b \leq T$ , and the value of  $\theta$  for all  $t \in [a, b]$  satisfies the following condition:

$$\theta_t < \tau, \quad \forall t \in [a, b]. \quad (2)$$

During the acceleration interval, we approximate the update trajectories of the current step using those of previous steps, allowing us to skip the calculations for these steps, as shown in Fig. 3a. Based on Local Transition Coherence, we propose a new training-free acceleration method called LTC-ACCEL, which improves the efficiency of the sampling process while maintaining the quality of the generated samples. It's important to note that Local Transition Coherence places no restrictions on the network's structure, meaning that LTC-ACCEL can be applied to nearly any diffusion model.

### 3.2. LTC-ACCEL: Transition Approximation

LTC-ACCEL reduces unnecessary computations by approximating the update trajectories of the current step using those from adjacent steps. In this section, we first introduce the formula for the approximated step. Next, we explain the conditions for this approximation and present the overall algorithm, followed by a description of the derivation.

**Definition 3.3.** With  $\phi(t)$  denoting the denoising progress at step  $t$ , the approximated step  $x_t^*$  of step  $t$  is defined as

$$\mathbf{x}_t^* = \mathbf{x}_{t+1} + w_g \gamma (\Delta \mathbf{x}_{t+2, t+1}), \quad (3)$$

where  $w_g = \frac{(\Delta \mathbf{x}_{t+1, t}) \cdot (\Delta \mathbf{x}_{t+2, t+1})}{\gamma \|\Delta \mathbf{x}_{t+2, t+1}\|^2}$ ,  $\gamma = \frac{\phi(t) - \phi(t+1)}{\phi(t+1) - \phi(t+2)}$ .

Here, we would like to emphasize that although the calculation of  $w_g$  relies on the target variable  $\mathbf{x}_t$ ,  $w_g$  itself is a convergent quantity that depends solely on the step  $t$ . To clearly identify the positions of the approximated steps, we define the acceleration condition:

**Definition 3.4.** The acceleration condition is defined as follows:

$$t \bmod r = r - 1, \quad (4)$$

where  $t$  is the step number, and  $r$  is a constant, mod stands for the modulo operation.

Based on these definitions, we propose LTC-ACCEL. During inference, following Eq. (2), we identify acceleration intervals. If the current step lies within an acceleration interval and satisfies the acceleration condition, we replace the original transition with the approximated step, as shown in Eq. (3). The detailed algorithm is presented in Algorithm 1.

#### 3.2.1. Formalizing $\gamma$ and $w_g$

In this section, we explain how to select  $\gamma$  and  $w_g$ , which are crucial for implementing LTC-ACCEL. The goal is to find appropriate values for  $w_g$  and  $\gamma$  that minimize the error of the approximated step, described as the difference between the approximated value  $\mathbf{x}_t^*$  and the target value  $\mathbf{x}_t$  as follows:

**Definition 3.5.** Parameter  $w_g$  and  $\gamma$  is defined as

$$w_g, \gamma = \underset{w_g, \gamma}{\operatorname{argmin}} \left( \|\Delta \mathbf{x}_{t+1, t} - w_g \gamma \Delta \mathbf{x}_{t+2, t+1}\|^2 \right). \quad (5)$$

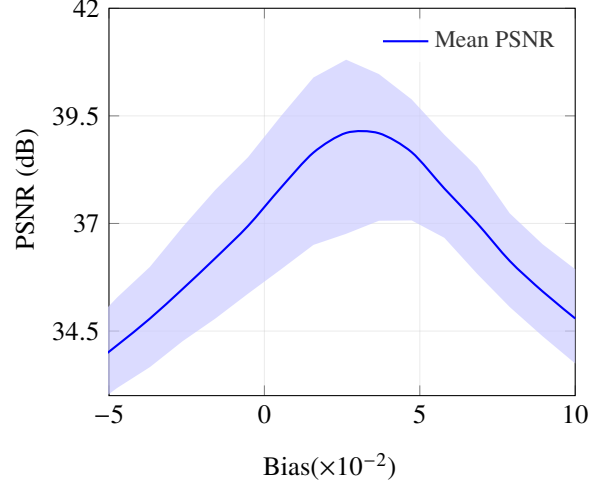


**Figure 4.** Variation of PSNR values between original images and those generated by LTC-ACCEL as a function of bias, following the same experimental setup as Fig. 3.

**Empirically determined value of  $\gamma$ :**  $\gamma$  controls the relative weighting of the step intervals, effectively adjusting the influence of denoising progress on the update process. We denote the denoising progress at step  $t$  as  $\phi(t)$  and define it as  $\phi(t) = \sqrt{\text{SNR}_t}$ , where SNR represents the signal-to-noise ratio. This choice is motivated by the observation that as denoising progresses, the signal becomes increasingly dominant over noise, leading to a higher SNR. Taking the square root of SNR provides a measure that scales more linearly with the improvement in signal quality, offering a practical representation of denoising progress. Consequently, we quantify the progress over the interval  $[t, t+1]$  as  $\phi(t) - \phi(t+1)$ , which serves as the foundation for defining  $\gamma$  as follows:

$$\gamma = \frac{\phi(t) - \phi(t+1)}{\phi(t+1) - \phi(t+2)}. \quad (6)$$

**Optimal of  $w_g$ :**  $w_g$  scales the magnitude of the transition operator. It is determined by minimizing the discrepancy between the actual transition and the approximated transition step, as given in Eq. (3). Here we provide the values of  $w_g$  as follows (see supplementary for details):

$$w_g = \frac{\Delta \mathbf{x}_{t+1, t} \cdot \Delta \mathbf{x}_{t+2, t+1}}{\gamma \|\Delta \mathbf{x}_{t+2, t+1}\|^2}. \quad (7)$$



### 3.2.2. Convergence analysis of $w_g$

As shown in Eq. (5), the calculation of  $w_g$  depends on  $\mathbf{x}_t$ . However, during sampling, the value of  $x_t$  is the target we aim to approximate, which poses a challenge to the approximation process. **Fortunately, we observe that  $w_g$  consistently exhibits convergence for across varying  $\mathbf{x}_t$ , allowing us to determine the corresponding  $w_g$  solely from  $t$ .** In this section, we first introduce the algorithm for evaluating  $w_g$ , and then employ it to conduct a rigorous convergence analysis of  $w_g$ .

**Algorithm for Estimating  $w_g$ :** Computing  $w_g$  is challenging because approximating  $\mathbf{x}_t$  introduces cumulative errors that propagate through subsequent steps, affecting the accuracy of the sampling process, as illustrated in Fig. 3b. To effectively mitigate this issue, we propose a two-step algorithm: 1) compute the current  $w_g$  and use it to derive the approximated step  $\mathbf{x}_t^*$ , which serves as the input for the next iteration; 2) perform a local search to optimize  $w_g$  across the entire acceleration interval, minimizing cumulative errors (see Algorithm 2 for details).

**Algorithm for Refining the Estimation of  $w_g$ :** Although the  $w_g$  obtained by Algorithm 2 performs well, we introduce an optional refinement step to further improve the fidelity of accelerated images. Specifically, we use PSNR to evaluate and enhance the quality of accelerated images. This metric quantifies fidelity by measuring the similarity between an accelerated image and its non-accelerated counterpart. Typically, a PSNR above 30 dB signifies high-fidelity generation. The refinement algorithm consists of: 1) introducing a bias to adjust all  $w_g$  values, and 2) conducting an end-to-end search within a predefined bias interval to determine the optimal adjustment (see Algorithm 3 for details).

**Analysis of results:** Similar to the convergence behavior observed in Fig. 3c, the  $w_g$  computed by Algorithm 2 consistently converges, ensuring the generality of our method (see supplementary for more details). Additionally, Fig. 4 demonstrates that introducing a bias further enhances image similarity, increasing the PSNR from 37.5 to 39. The symmetry observed between bias and PSNR allows efficient optimization through binary search.

### 3.3. Error Analysis of the Approximated Step

In this section, we demonstrate that the error introduced by the approximation is generally negligible. We first provide the upper bound of the error of approximating a single step, followed by a comprehensive evaluation of the actual error incurred throughout the sampling process in practice.

**Error of approximating a single step:** Using the expressions for  $w_g$  and  $\gamma$ , we can estimate the relative error between the approximated step and the original step. When the angle between  $\Delta\mathbf{x}_{t+1,t}$  and  $\Delta\mathbf{x}_{t+2,t+1}$  is less than a threshold  $\tau$ , the relative error  $\epsilon_r$  can be expressed as follows (see

supplementary for details):

$$\epsilon_r = \frac{\|\mathbf{x}_t - \mathbf{x}_t^*\|^2}{\|\Delta\mathbf{x}_{t+1,t}\|^2} < \tau^2. \quad (8)$$

This implies that the relative error introduced by the approximate step is smaller than the update term of the original process, scaled by  $\tau^2$ . When  $\tau$  is typically on the order of magnitude of  $[0.1, 0.2]$ ,  $\epsilon_r$  becomes negligible.

---

#### Algorithm 1 LTC-ACCEL Acceleration

---

```

1: Input: Diffusion model  $p_\theta$ , acceleration interval  $[a, b]$ ,
   acceleration cycle  $r$ , mapping  $\phi$ , constant sequence  $w_g$ ,
   initial noise  $\mathbf{x}_N$ .
2: Output:  $\mathbf{x}_0$ .
3: for  $t = N$  to 0 do
4:   if  $t \in [a, b]$  and  $t \bmod r = r - 1$  then
5:      $\gamma = \frac{\phi(r) - \phi(r+1)}{\phi(r+1) - \phi(r+2)}$ 
6:      $\mathbf{x}_t = \mathbf{x}_{t+1} + w_g[t] \cdot \gamma \cdot \Delta\mathbf{x}_{t+2,t+1}$ 
7:   else
8:      $\mathbf{x}_t = p_\theta(\mathbf{x}_{t+1}, t)$ 
9:   end if
10: end for
11: return  $\mathbf{x}_0$ 

```

---



---

#### Algorithm 2 Calculate $w_g$

---

```

1: Input: Diffusion model  $p_\theta$ , acceleration interval  $[a, b]$ ,
   acceleration cycle  $r$ , mapping  $\phi$ , initial noise  $\mathbf{x}_N$ .
2: Output:  $w_g$ .
3: for  $t = N$  to 0 do
4:   if  $t \in [a, b]$  and  $t \bmod r = r - 1$  then
5:      $\gamma = \frac{\phi(t) - \phi(t+1)}{\phi(t+1) - \phi(t+2)}$ 
6:      $w_g[t] = \frac{\Delta\mathbf{x}_{t+1,t} \cdot \Delta\mathbf{x}_{t+2,t+1}}{\gamma \|\Delta\mathbf{x}_{t+2,t+1}\|^2}$ 
7:      $\mathbf{x}_t^* = \mathbf{x}_{t+1} + w_g \gamma (\Delta\mathbf{x}_{t+2,t+1})$ 
8:      $\mathbf{x}_t = \mathbf{x}_t^*$ 
9:   else
10:     $\mathbf{x}_t = p_\theta(\mathbf{x}_{t+1}, t)$ 
11:   end if
12: end for
13: return  $w_g$ 

```

---

**Error in practice:** As the approximation of steps extends to  $N$  steps during inference, the error accumulates, leading to the results shown in the figure. The findings indicate that even when 32.5% of the steps are approximated, the resulting error remains only 6.0%, demonstrating that the error is nearly imperceptible. Notably, our method, LTC-ACCEL, achieves a PSNR of 36.6, as illustrated in Fig. 4.

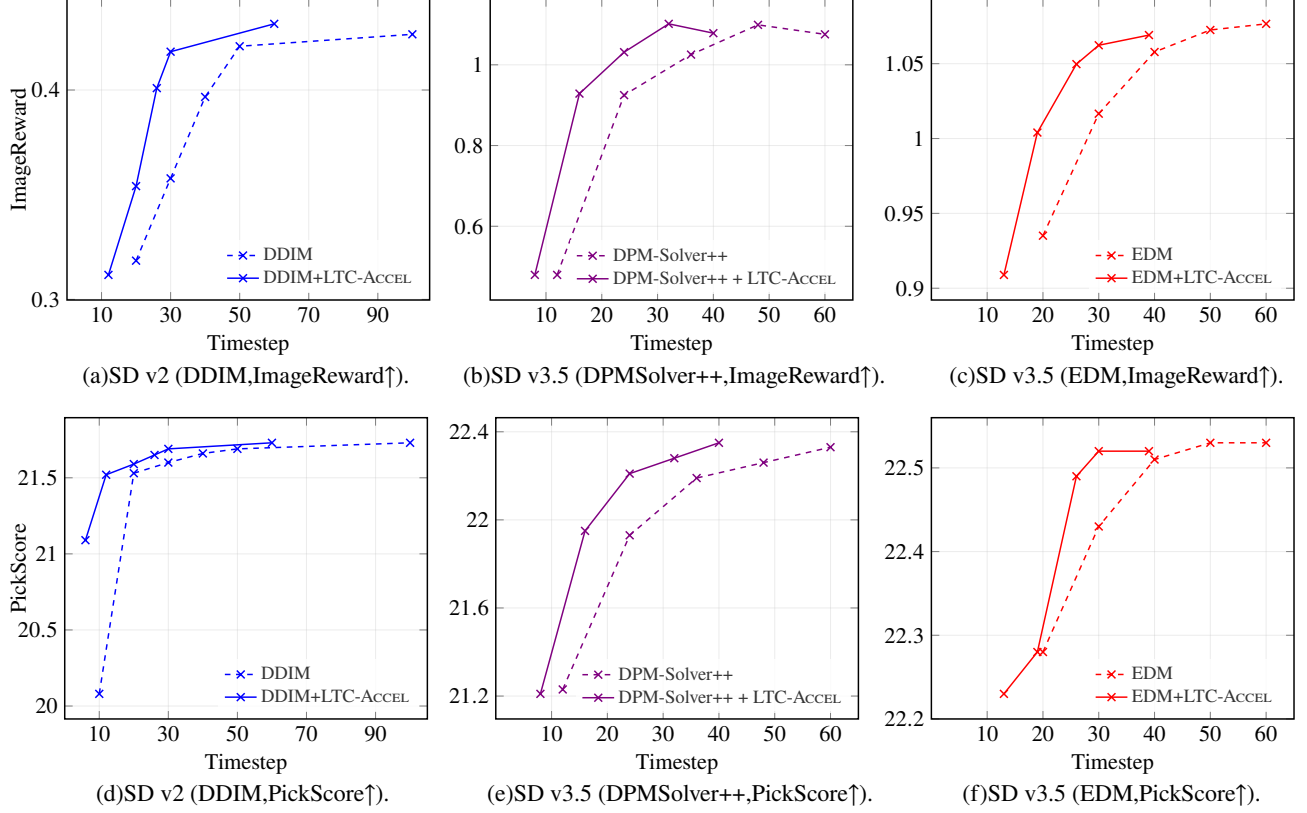


**Figure 5.** Quantitative results of text-to-image. We present our results on **Stable Diffusion v2** and **Stable Diffusion v3.5** by measuring the ImageReward and PickScore using 1000 prompt-image pairs. To demonstrate our compatibility with most schedulers, we use DDIM for sampling on Stable Diffusion v2, DPM-Solver++ and EDM for sampling on Stable Diffusion v3.5. The results demonstrate that our method achieves a **1.67× acceleration** on Stable Diffusion v3.5, as well as a **1.67× acceleration** on Stable Diffusion v2.

---

#### Algorithm 3 (Optional) Improve $w_g$

---

- 1: **Input:** Diffusion model  $p_\theta$ , free ride  $p_\theta^*$ , bias interval  $[c, d]$ , noise  $x_0$ .
  - 2: **Output:** Constant  $bias^*$ .
  - 3:  $\mathbf{x}_0 = \prod_{t=N}^0 p_\theta(\mathbf{x}_{t+1}, t)$
  - 4:  $bias^* = \underset{bias \in [c, d]}{\operatorname{argmax}} (\operatorname{PSNR}(x_N, \prod_{t=N}^0 p_\theta^*(\mathbf{x}_{t+1}, t, w_g + bias))$
  - 5: **return**  $bias^*$
- 

## 4. Experiments

In this section, we conduct extensive experiments to validate our method’s effectiveness. First, in Sec. 4.1, we provide an overview of the experimental setup. Then, in Sec. 4.2 and Sec. 4.3, we present a comprehensive evaluation of text-to-image and text-to-video synthesis. In Sec. 4.4, we assess the integration of our method with other methods. Finally, in Sec. 4.5, we conduct ablation studies to further validate our method’s effectiveness and potential.

### 4.1. Experimental Settings

In all experiments, unless otherwise specified, we use a classifier-free guidance [5] intensity of 7.5 without additional enhancement techniques. To evaluate acceleration performance, we perform inference in float16 and measure speedup based on the number of inference steps. Additionally, we set  $\phi(t)$ , as mentioned in Sec. 3.2, to the  $\sqrt{\operatorname{SNR}_t}$  values of the current step. All experiments are conducted without any additional training and we ensure that both the original model and LTC-Accel start with consistent initial noise. In addition, for each prompt, we sample a unique starting noise to ensure variability.

### 4.2. Text-to-image Synthesis Task

In this section, we evaluate the performance of LTC-Accel in text-to-image synthesis task.

**Settings:** We first introduce the configurations used for evaluation in this section: **1) Baselines:** DDIM for Stable Diffusion v2 [36], EDM [8] and DPM-Solver++ [22] for Stable Diffusion v3.5-mid [3]. **2) Datasets:** We employ the random 1,000 prompts from the MS-COCO 2017 dataset [21]

Model	DeepCache			LTC-ACCEL			Acceleration Condition	Speedup
	Steps	Time(ms)	ImageReward↑	Steps	Time(ms)	ImageReward↑		
SD v2	10	264	-0.2246	8	208	-0.2739	$t \bmod r = r - 3, t > 4$	1.25×
	20	524	0.2445	16	419	<b>0.2456</b>	$t \bmod r = r - 3, t > 8$	1.25×
	50	1411	0.4039	38	1038	<b>0.4096</b>	$t \bmod r = r - 3, t > 12$	1.41×
	100	3014	0.4242	75	2171	<b>0.4246</b>	$t \bmod r = r - 3, 24 < t \leq 90$	1.38×

**Table 1.** Quantitative Evaluation of Text-to-Image Generation via DDIM Sampling with **LTC-ACCEL** and **DeepCache**. In this experiment, the parameter  $N$  of DeepCache is set to  $N = 2$ , and the period parameter  $r$  is set to  $r = 3$ . The results are bold if they are better both in speed and quality. The results demonstrate that our method can be combined with DeepCache, achieving an **additional 1.41× acceleration** on top of DeepCache’s speedup.

Model	Original		Ays		LTC-ACCEL		Speedup
	Steps	ImageReward↑	Steps	ImageReward↑	Steps	ImageReward↑	
SD v1.5	10	0.1111	10	0.1332	8	0.1309	1.25×

**Table 2.** Quantitative Evaluation of Text-to-Image Generation via DPM-Solver++ Sampling with **LTC-ACCEL** and **Align Your Steps**. The results demonstrate that our method can be integrated with Align Your Steps, achieving a **1.25× acceleration** with minimal impact on the generation quality.

for Stable Diffusion v2 trials, and Stable Diffusion v3.5-mid. **3) Metrics:** In our experiments with Stable Diffusion v2 and v3.5-mid, we used the ImageReward metric [50] and PickScore [13]. ImageReward is a model trained on human comparisons to evaluate text-to-image synthesis, considering factors like alignment with text and aesthetic quality. PickScore, based on CLIP and trained on the Pick-a-Pic dataset, predicts user preferences for generated images.

**Results:** Fig. 5 presents the acceleration results from our experiments. LTC-ACCEL demonstrates consistently strong performance across different text-to-image models and sampling methods. In particular, we obtain a 1.67× speedup on Stable Diffusion v2 and v3.5, which is notably high for a training-free method.

### 4.3. Text-to-video Synthesis Task

In this section, we evaluate the performance of LTC-ACCEL on several video models in the text-to-video synthesis task.

**Settings:** The configurations used for evaluation are as follows: **1) Baselines:** We use Anime-Diff [4] and CogVideoX [53] 2B as baselines, with epiCRealism [2] as the base model for Anime-Diff. **2) Datasets:** We randomly select 100 prompts from the MS-COCO 2017 dataset [21]. **3) Metrics:** Following prior work [48], we evaluate video quality using Frame Consistency and Textual Faithfulness. Specifically, for Frame Consistency, we compute CLIP image embeddings for each frame and report the average cosine similarity across all frame pairs. For Textual Faithfulness, we compute the average ImageReward score between each frame and its corresponding text prompt.

**Results:** As shown in Tab. 3, LTC-ACCEL obtains promising

results across different video generation models. Notably, it can even achieve a 1.54× speedup with almost no impact on video generation quality.

### 4.4. Compatibility with Other acceleration methods

Since LTC-ACCEL leverages the relationship between the network’s output, it introduces a completely new approach to acceleration. This makes it compatible with a wide variety of both training-based and training-free methods. In this section, we combine LTC-ACCEL with various existing acceleration methods, both training-free and training-based, for text-to-image and text-to-video tasks.

#### 4.4.1. Combined with Training-Free Methods

In this part, our sampler configurations are meticulously set up as follows: **1) Baselines:** We select DeepCache, Align Your Steps, and INT8 quantization as representatives of training-free methods and conduct experiments on Stable Diffusion v2. Specifically, DeepCache is a novel training-free method that accelerates diffusion models by leveraging temporal redundancy in the denoising process to cache and reuse features, while Align Your Steps is a principled method for optimizing sampling schedules in diffusion models, particularly efficient in few-step synthesis. INT8 quantization converts high-precision model parameters to 8-bit integers, accelerating video processing and inference while maintaining acceptable quality. **2) Datasets:** The random 1,000 prompts from the MS-COCO 2017. **3) Metrics:** ImageReward introduced in Sec. 4.2.

**Results:** Tab. 1 shows the results of combining our method with DeepCache, achieving a 2.3× speedup compared to the



Model	Original			LTC-ACCEL			Speedup
	Steps	Text↑	Smooth↑	Steps	Text↑	Smooth↑	
Anime-diff	10	0.2439	0.9713	7	0.2426	0.9700	1.43×
Anime-diff	20	0.3050	0.9729	13	0.2939	<b>0.9732</b>	1.54×
Anime-diff	30	0.3662	0.9676	19	0.3465	<b>0.9681</b>	1.58×
CogVideoX 2B	20	-0.1441	0.9442	14	-0.1673	0.9361	1.43×
CogVideoX 2B	30	0.2302	0.9464	19	<b>0.2320</b>	0.9435	1.58×
CogVideoX 2B	40	0.3918	0.9514	26	0.3775	0.9511	1.54×
CogVideoX 2B (int8)	40	0.2113	0.9456	26	0.2010	0.9449	1.54×

**Table 3.** Quantitative results of text-to-video, comparing **Original** and **LTC-ACCEL** settings. Text and Smooth denote Textual Faithfulness and Frame Consistency, respectively. The results are bold if they are better both in speed and quality. The results demonstrate that our method can be combined with video models well, achieving a **1.58× acceleration** at most.

Model	Original			Distillation			LTC-ACCEL			Speedup
	Steps	Text↑	Smooth↑	Steps	Text↑	Smooth↑	Steps	Text↑	Smooth↑	
Anime-diff-lightning	4	0.3662	0.9685	3	0.2913	0.9673	3	0.3550	0.9645	1.33×
Anime-diff-lightning	8	0.3371	0.9697	5	0.2978	0.9690	5	<b>0.3493</b>	0.9654	1.60×

**Table 4.** Quantitative results of text-to-video, comparing **Anime-diff-lightning (original steps)**, **Anime-diff-lightning (same steps as LTC-ACCEL)**, and **LTC-ACCEL**. The results are bold if they are better both in speed and quality. The results demonstrate that our method can be integrated with Anime-diff-lightning, achieving an **additional 1.60× acceleration** with minimal impact on the generation quality.

original model, and even improving the generation quality in terms of ImageReward when combined with our method. In addition, Tab. 2 shows the results of combining our method with Align Your Steps, where 8 steps achieved the same effect as Align Your Steps with 10 steps, and the performance difference between the two is only 0.0023. This small difference is negligible compared to the original process without applying Align Your Steps to improve the scheduler. Moreover, we show that our approach is compatible with quantization techniques, successfully applying INT8 quantization to CogVideoX as shown in Tab. 3.

#### 4.4.2. Combined with Training-Based Methods

In particular, considering the setup of the distilled model, we do not use classifier-free guidance in this section. Our sampler configurations are meticulously set up as follows: **1) Baselines:** We use Anime-Diff-Lightning as a representative of distilled models. Anime-diff-lightning [20] is a distilled version of the anime-diff model, designed to retain core functionality while optimizing performance. Specifically, we use the 8-step and 4-step weights of Anime-Diff-Lightning, where the 8-step weights correspond to 8-step inference and the 4-step weights correspond to 4-step inference. **2) Datasets:** The random 100 prompts from the MS-COCO 2017 dataset [21]. **3) Metrics:** Frame Consistency and Textual Faithfulness introduced in Sec. 4.3.

**Results:** The results in Tab. 4 show that our model can effectively accelerate distilled models, and even speed up

the 4-step model to 3 steps with minimal impact on video generation quality, when compared to the original process with the same computational cost.

#### 4.5. Ablation Studies

In this section, we perform ablation studies to further assess and validate the effectiveness of our method.

**Directly Skipping Steps:** We compare our approach with the Skipping Steps strategy within the same acceleration framework. Tab. 5 shows that our method improves computational efficiency over the original approach while preserving generation quality better than the Skipping Steps.

Model	Scheduler	Skipping Steps		LTC-ACCEL	
		Steps	ImageReward↑	Steps	ImageReward↑
SD v2	DDIM	7	0.0537	7	0.1472
	DDIM	10	0.2003	10	0.2442
	DDIM	13	0.2812	13	0.3129
SD v2	EDM	7	0.0158	7	0.2018
	EDM	10	0.2003	10	0.3171
	EDM	13	0.2582	13	0.3335

**Table 5.** Ablation study comparing LTC-ACCEL with the **Skipping Steps** method under the same acceleration framework. The results show that LTC-ACCEL outperforms Skipping Steps, indicating the effectiveness of LTC-ACCEL. The results demonstrate that our method **consistently outperforms** the Skipping Steps strategy in all scenarios.

## 5. Conclusion

We introduce LTC-ACCEL, a training-free method that accelerates diffusion sampling via the Local Transition Coherence phenomenon. It reduces computation, preserves fidelity, and integrates well with existing acceleration techniques.

**Limitations:** Our method has two main limitations. First, its effectiveness relies on the Local Transition Coherence phenomenon, which weakens with very few sampling steps (e.g., under three). Second, while training-free, it requires careful hyperparameter tuning for optimal acceleration, as suitable intervals vary across diffusion processes.

## References

- [1] Prafulla Dhariwal and Alexander Nichol. Diffusion models beat gans on image synthesis. In *NeurIPS*, 2021. 1
- [2] Epinikion. epicrealism. <https://civitai.com/models/25694>. Accessed: 2023. 7
- [3] Patrick Esser, Sumith Kulal, Andreas Blattmann, Rahim Entezari, Jonas Müller, Harry Saini, Yam Levi, Dominik Lorenz, Axel Sauer, Frederic Boesel, Dustin Podell, Tim Dockhorn, Zion English, Kyle Lacey, Alex Goodwin, Yannik Marek, and Robin Rombach. Scaling rectified flow transformers for high-resolution image synthesis, 2024. 6, 1
- [4] Yuwei Guo, Ceyuan Yang, Anyi Rao, Zhengyang Liang, Yao-hui Wang, Yu Qiao, Maneesh Agrawala, Dahua Lin, and Bo Dai. Animatediff: Animate your personalized text-to-image diffusion models without specific tuning. *arXiv preprint arXiv:2307.04725*, 2023. 1, 2, 7, II
- [5] Jonathan Ho and Tim Salimans. Classifier-free diffusion guidance. *arXiv preprint arXiv:2207.12598*, 2022. 2, 3, 6
- [6] Jonathan Ho, Ajay Jain, and Pieter Abbeel. Denoising diffusion probabilistic models. *NeurIPS*, 2020. 1
- [7] Peng Huang, Xue Gao, Lihong Huang, Jing Jiao, Xiaokang Li, Yuanyuan Wang, and Yi Guo. Chest-diffusion: A light-weight text-to-image model for report-to-cxr generation. *IEEE*, 2024. 1
- [8] Tero Karras, Miika Aittala, Timo Aila, and Samuli Laine. Elucidating the design space of diffusion-based generative models. *NeurIPS*, 2022. 3, 6, II
- [9] Tero Karras, Miika Aittala, Jaakko Lehtinen, Janne Hellsten, Timo Aila, and Samuli Laine. Analyzing and improving the training dynamics of diffusion models. In *CVPR*, 2024. 1
- [10] Tero Karras, Miika Aittala, Tuomas Kynkäänniemi, Jaakko Lehtinen, Timo Aila, and Samuli Laine. Guiding a diffusion model with a bad version of itself. *NeurIPS*, 2025. 2, 3
- [11] Bosung Kim, Kyuhwan Lee, Isu Jeong, Jungmin Cheon, Yeojin Lee, and Seulki Lee. On-device sora: Enabling diffusion-based text-to-video generation for mobile devices. *arXiv preprint arXiv:2502.04363*, 2025. 1
- [12] Dongjun Kim, Chieh-Hsin Lai, Wei-Hsiang Liao, Naoki Murata, Yuhta Takida, Toshimitsu Uesaka, Yutong He, Yuki Mitsufuji, and Stefano Ermon. Consistency trajectory models: Learning probability flow ode trajectory of diffusion. *arXiv preprint arXiv:2310.02279*, 2023. 1, 2
- [13] Yuval Kirstain, Adam Polyak, Uriel Singer, Shahbuland Matiana, Joe Penna, and Omer Levy. Pick-a-pic: An open dataset of user preferences for text-to-image generation. In *NeurIPS*, 2023. 7
- [14] Zhifeng Kong, Wei Ping, Jiayi Huang, Kexin Zhao, and Bryan Catanzaro. Diffwave: A versatile diffusion model for audio synthesis, 2021. 1
- [15] Raghuraman Krishnamoorthi. Quantizing deep convolutional networks for efficient inference: A whitepaper. *arXiv preprint arXiv:1806.08342*, 2018. 1
- [16] Taegyeong Lee, Soyeong Kwon, and Taehwan Kim. Grid diffusion models for text-to-video generation. *IEEE*, 2024. 1
- [17] Jean-Marie Lemerrier, Julius Richter, Simon Welker, and Timo Gerkmann. Storm: A diffusion-based stochastic regeneration model for speech enhancement and dereverberation. *IEEE/ACM Transactions on Audio, Speech, and Language Processing*, 2023. 1
- [18] Chenda Li, Samuele Cornell, Shinji Watanabe, and Yanmin Qian. Diffusion-based generative modeling with discriminative guidance for streamable speech enhancement. In *2024 IEEE Spoken Language Technology Workshop (SLT)*. IEEE, 2024. 1
- [19] Youwei Liang, Junfeng He, Gang Li, Peizhao Li, Arseniy Klimovskiy, Nicholas Carolan, Jiao Sun, Jordi Pont-Tuset, Sarah Young, Feng Yang, et al. Rich human feedback for text-to-image generation. In *CVPR*, 2024. 1
- [20] Shanchuan Lin and Xiao Yang. Animatediff-lightning: Cross-model diffusion distillation. *arXiv preprint arXiv:2403.12706*, 2024. 1, 2, 8, II
- [21] Tsung-Yi Lin, Michael Maire, Serge Belongie, James Hays, Pietro Perona, Deva Ramanan, Piotr Dollár, and C Lawrence Zitnick. Microsoft coco: Common objects in context. In *ECCV*, 2014. 6, 7, 8
- [22] Cheng Lu, Yuhao Zhou, Fan Bao, Jianfei Chen, Chongxuan Li, and Jun Zhu. Dpm-solver++: Fast solver for guided sampling of diffusion probabilistic models. *arXiv preprint arXiv:2211.01095*, 2022. 2, 3, 6, I
- [23] Cheng Lu, Yuhao Zhou, Fan Bao, Jianfei Chen, Chongxuan Li, and Jun Zhu. Dpm-solver: A fast ode solver for diffusion probabilistic model sampling in around 10 steps. *NeurIPS*, 2022. 2, 3
- [24] Yen-Ju Lu, Zhong-Qiu Wang, Shinji Watanabe, Alexander Richard, Cheng Yu, and Yu Tsao. Conditional diffusion probabilistic model for speech enhancement. In *ICASSP 2022-2022 IEEE International Conference on Acoustics, Speech and Signal Processing (ICASSP)*. Ieee, 2022. 1
- [25] Simian Luo, Yiqin Tan, Longbo Huang, Jian Li, and Hang Zhao. Latent consistency models: Synthesizing high-resolution images with few-step inference. *arXiv preprint arXiv:2310.04378*, 2023. 1, 2
- [26] Xinyin Ma, Gongfan Fang, and Xinchao Wang. Deepcache: Accelerating diffusion models for free. *IEEE*, 2023. 2, 3, II
- [27] Alexander Quinn Nichol and Prafulla Dhariwal. Improved denoising diffusion probabilistic models. In *ICML*, 2021. 1
- [28] Gyeongrok Oh, Jaehwan Jeong, Sieun Kim, Wonmin Byeon, Jinkyu Kim, Sungwoong Kim, and Sangpil Kim. Mevg: Multi-event video generation with text-to-video models. In *ECCV*, 2025. 1

- [29] William Peebles and Saining Xie. Scalable diffusion models with transformers. In *ICCV*, 2023. 1
- [30] Dustin Podell, Zion English, Kyle Lacey, Andreas Blattmann, Tim Dockhorn, Jonas Müller, Joe Penna, and Robin Rombach. Sdxl: Improving latent diffusion models for high-resolution image synthesis. *arXiv preprint arXiv:2307.01952*, 2023. 1
- [31] Fan Qi, Yu Duan, Huaiwen Zhang, and Changsheng Xu. Sign-gen: End-to-end sign language video generation with latent diffusion. In *ECCV*, 2025. 1
- [32] Yurui Qian, Qi Cai, Yingwei Pan, Yehao Li, Ting Yao, Qibin Sun, and Tao Mei. Boosting diffusion models with moving average sampling in frequency domain. In *CVPR*, 2024. 2, 3
- [33] Ilija Radosavovic, Raj Prateek Kosaraju, Ross Girshick, Kaiming He, and Piotr Dollar. Designing network design spaces. In *CVPR*, 2020. 1
- [34] Julius Richter, Simon Welker, Jean-Marie Lemerrier, Bunlong Lay, and Timo Gerkmann. Speech enhancement and dereverberation with diffusion-based generative models. *IEEE/ACM Transactions on Audio, Speech, and Language Processing*, 2023. 1
- [35] Robin Rombach, Andreas Blattmann, Dominik Lorenz, Patrick Esser, and Björn Ommer. High-resolution image synthesis with latent diffusion models. In *CVPR*, 2022. 2
- [36] Robin Rombach, Andreas Blattmann, Dominik Lorenz, Patrick Esser, and Björn Ommer. High-resolution image synthesis with latent diffusion models. In *CVPR*, 2022. 6, 11
- [37] Amirmojtaba Sabour, Sanja Fidler, and Karsten Kreis. Align your steps: Optimizing sampling schedules in diffusion models. *arXiv preprint arXiv:2404.14507*, 2024. 2, 3
- [38] Tim Salimans and Jonathan Ho. Progressive distillation for fast sampling of diffusion models. *arXiv preprint arXiv:2202.00512*, 2022. 1, 2
- [39] Mark Sandler, Andrew Howard, Menglong Zhu, Andrey Zhmoginov, and Liang Chieh Chen. Mobilenetv2: Inverted residuals and linear bottlenecks. *IEEE*, 2018. 1, 2
- [40] Axel Sauer, Dominik Lorenz, Andreas Blattmann, and Robin Rombach. Adversarial diffusion distillation. In *ECCV*, 2024. 1, 2
- [41] Jiaming Song, Chenlin Meng, and Stefano Ermon. Denoising diffusion implicit models. *arXiv preprint arXiv:2010.02502*, 2020. 1, 3, 1
- [42] Yang Song, Prafulla Dhariwal, Mark Chen, and Ilya Sutskever. Consistency models. In *ICML*, 2023. 1, 2
- [43] Ahmad Süleyman and Göksel Biricik. Grounding text-to-image diffusion models for controlled high-quality image generation. *arXiv preprint arXiv:2501.09194*, 2025. 1
- [44] Wan Team. Wan: Open and advanced large-scale video generative models. 2025. 1
- [45] Thanapat Trachu, Chawan Piansaddhayanon, and Ekapol Chuangsuwanich. Thunder: Unified regression-diffusion speech enhancement with a single reverse step using brownian bridge. *arXiv preprint arXiv:2406.06139*, 2024. 1
- [46] Simon Welker, Julius Richter, and Timo Gerkmann. Speech enhancement with score-based generative models in the complex stft domain. *arXiv preprint arXiv:2203.17004*, 2022. 1
- [47] Felix Wimbauer, Bichen Wu, Edgar Schoenfeld, Xiaoliang Dai, Ji Hou, Zijian He, Artsiom Sanakoyeu, Peizhao Zhang, Sam Tsai, Jonas Kohler, et al. Cache me if you can: Accelerating diffusion models through block caching. In *CVPR*, 2024. 2, 3
- [48] Jay Zhangjie Wu, Yixiao Ge, Xintao Wang, Stan Weixian Lei, Yuchao Gu, Yufei Shi, Wynne Hsu, Ying Shan, Xiaohu Qie, and Mike Zheng Shou. Tune-a-video: One-shot tuning of image diffusion models for text-to-video generation. In *ICCV*, 2023. 7
- [49] Changming Xiao, Qi Yang, Feng Zhou, and Changshui Zhang. From text to mask: Localizing entities using the attention of text-to-image diffusion models. *Neurocomputing*, 2024. 1
- [50] Jiazheng Xu, Xiao Liu, Yuchen Wu, Yuxuan Tong, Qinkai Li, Ming Ding, Jie Tang, and Yuxiao Dong. Imagereward: Learning and evaluating human preferences for text-to-image generation. *NeurIPS*, 2023. 7
- [51] Shuchen Xue, Zhaoqiang Liu, Fei Chen, Shifeng Zhang, Tianyang Hu, Enze Xie, and Zhenguo Li. Accelerating diffusion sampling with optimized time steps. In *CVPR*, 2024. 2, 3
- [52] Ruihan Yang, Prakhar Srivastava, and Stephan Mandt. Diffusion probabilistic modeling for video generation. *Entropy; International and Interdisciplinary Journal of Entropy and Information Studies*, 2023. 1
- [53] Zhuoyi Yang, Jiayan Teng, Wendi Zheng, Ming Ding, Shiyu Huang, Jiazheng Xu, Yuanming Yang, Wenyi Hong, Xiaohan Zhang, Guanyu Feng, et al. Cogvideox: Text-to-video diffusion models with an expert transformer. *arXiv preprint arXiv:2408.06072*, 2024. 1, 7
- [54] Tianwei Yin, Michaël Gharbi, Richard Zhang, Eli Shechtman, Fredo Durand, William T Freeman, and Taesung Park. One-step diffusion with distribution matching distillation. In *CVPR*, 2024. 1, 2
- [55] Xiangyu Zhang, Xinyu Zhou, Mengxiao Lin, and Jian Sun. Shufflenet: An extremely efficient convolutional neural network for mobile devices. In *CVPR*, 2018. 1, 2
- [56] Wenliang Zhao, Lujia Bai, Yongming Rao, Jie Zhou, and Jiwen Lu. Unipc: A unified predictor-corrector framework for fast sampling of diffusion models. *NeurIPS*, 2023. 3
- [57] Yang Zhao, Yanwu Xu, Zhisheng Xiao, Haolin Jia, and Tingbo Hou. Mobilediffusion: Instant text-to-image generation on mobile devices. In *ECCV*. Springer, 2024. 1
- [58] Kaiwen Zheng, Cheng Lu, Jianfei Chen, and Jun Zhu. Dpm-solver-v3: Improved diffusion ode solver with empirical model statistics. *NeurIPS*, 2023. 2, 3
- [59] Mingyuan Zhou, Huangjie Zheng, Zhendong Wang, Mingzhang Yin, and Hai Huang. Score identity distillation: Exponentially fast distillation of pretrained diffusion models for one-step generation. In *ICML*, 2024. 1, 2
- [60] Zhenyu Zhou, Defang Chen, Can Wang, and Chun Chen. Fast ode-based sampling for diffusion models in around 5 steps. In *CVPR*, 2024. 3



## Supplementary Material

### Overview

The supplementary materials consist of three sections:

- **The first section is the Mathematical Derivation of LTC-ACCEL** (see Appendix A) The overall mathematical derivation consists of two parts:
  - We present the derivation process of  $w_g$  in detail (see Appendix A.1).
  - We introduce the derivation process for the error upper bound inequality in detail (see Appendix A.2).
  - We provide additional experimental evidence demonstrating the convergence of  $w_g$  and show that this convergence holds across different schedulers (see Appendix A.3).
- **The second section details the experimental setup for the figures** (see Appendix B).
- **The final section focuses on providing detailed experimental settings** (see Appendix C), including three parts:
  - We provide the details of the acceleration interval and the conditions for setting the approximated steps (see Appendix C.1).
  - We specify which experiments utilized the optional algorithm and which did not (see Appendix C.2).
  - We present intuitive experimental visual results to demonstrate the effectiveness of our LTC-ACCEL (see Appendix D).

### A. Mathematical Derivation

#### A.1. Derivation of $w_g$

To derive the  $w_g$ , we have:

$$w_g = \arg \min \left( \left\| \Delta \mathbf{x}_{t+1,t} - w_g \gamma \Delta \mathbf{x}_{t+2,t+1} \right\|^2 \right). \quad (9)$$

We expand the objective function in terms of the inner product:

$$\begin{aligned} & \left\| \Delta \mathbf{x}_{t+1,t} - w_g \gamma \Delta \mathbf{x}_{t+2,t+1} \right\|^2 \\ &= \left\| \Delta \mathbf{x}_{t+1,t} \right\|^2 - 2w_g \gamma (\Delta \mathbf{x}_{t+1,t} \cdot \Delta \mathbf{x}_{t+2,t+1}) \\ & \quad + w_g^2 \gamma^2 \left\| \Delta \mathbf{x}_{t+2,t+1} \right\|^2. \end{aligned} \quad (10)$$

Taking the derivative of this expression with respect to  $w_g$  and setting it equal to zero yields:

$$\begin{aligned} & \frac{\partial}{\partial w_g} \left[ \left\| \Delta \mathbf{x}_{t+1,t} - w_g \gamma \Delta \mathbf{x}_{t+2,t+1} \right\|^2 \right] \\ &= -2\gamma (\Delta \mathbf{x}_{t+1,t} \cdot \Delta \mathbf{x}_{t+2,t+1}) + 2w_g \gamma^2 \left\| \Delta \mathbf{x}_{t+2,t+1} \right\|^2 \\ &= 0. \end{aligned} \quad (11)$$

Rearranging this equation, we obtain:

$$w_g \gamma \left\| \Delta \mathbf{x}_{t+2,t+1} \right\|^2 = \Delta \mathbf{x}_{t+1,t} \cdot \Delta \mathbf{x}_{t+2,t+1}. \quad (12)$$

Thus, the final expression for  $w_g$  is given by:

$$w_g = \frac{\Delta \mathbf{x}_{t+1,t} \cdot \Delta \mathbf{x}_{t+2,t+1}}{\gamma \left\| \Delta \mathbf{x}_{t+2,t+1} \right\|^2}. \quad (13)$$

#### A.2. Derivation of the Error Upper Bound Inequality

To derive the inequality, we have:

$$\theta = \arccos \left( \frac{\Delta \mathbf{x}_{t+1,t} \cdot \Delta \mathbf{x}_{t+2,t+1}}{\left\| \Delta \mathbf{x}_{t+1,t} \right\|^2 \left\| \Delta \mathbf{x}_{t+2,t+1} \right\|^2} \right) < \tau, \quad (14)$$

which is equivalent to:

$$\frac{\Delta \mathbf{x}_{t+1,t} \cdot \Delta \mathbf{x}_{t+2,t+1}}{\left\| \Delta \mathbf{x}_{t+1,t} \right\|^2 \left\| \Delta \mathbf{x}_{t+2,t+1} \right\|^2} > \cos \tau. \quad (15)$$

Substituting this back into Eq. (9), we get:

$$\left\| \Delta \mathbf{x}_{t+1,t} \right\|^2 - \frac{(\Delta \mathbf{x}_{t+1,t} \cdot \Delta \mathbf{x}_{t+2,t+1})^2}{\left\| \Delta \mathbf{x}_{t+2,t+1} \right\|^2}. \quad (16)$$

Squaring both sides of the inequality and substituting the expressions, we can derive:

$$\begin{aligned} & \left\| \Delta \mathbf{x}_{t+1,t} - w_g \gamma \Delta \mathbf{x}_{t+2,t+1} \right\|^2 \\ & \leq \left\| \Delta \mathbf{x}_{t+1,t} \right\|^2 (1 - \cos^2 \tau) \\ & = \left\| \Delta \mathbf{x}_{t+1,t} \right\|^2 \sin^2 \tau \\ & \leq \left\| \Delta \mathbf{x}_{t+1,t} \right\|^2 \tau^2. \end{aligned} \quad (17)$$

#### A.3. Experimental Verification of $w_g$ Convergence

We select DPM-Solver++ [22] and DDIM [41] as representative schedulers for our experiments on Stable Diffusion v2. Given that  $w_g$  tends to exhibit stronger convergence with more steps, we choose 20 steps as a representative case. Fig. 6a and Fig. 6c illustrate the convergence behavior of the original  $w_g$ , while Fig. 6b and Fig. 6d demonstrate that the  $w_g$  values obtained through our algorithm also exhibit convergence.

### B. Experimental Setup for Figures

In this section, we provide the experimental settings for all figures presented in the main text.

#### • Figure 1

- The base model is Stable Diffusion v3.5 [3], and the corresponding scheduler is DPM-Solver++.

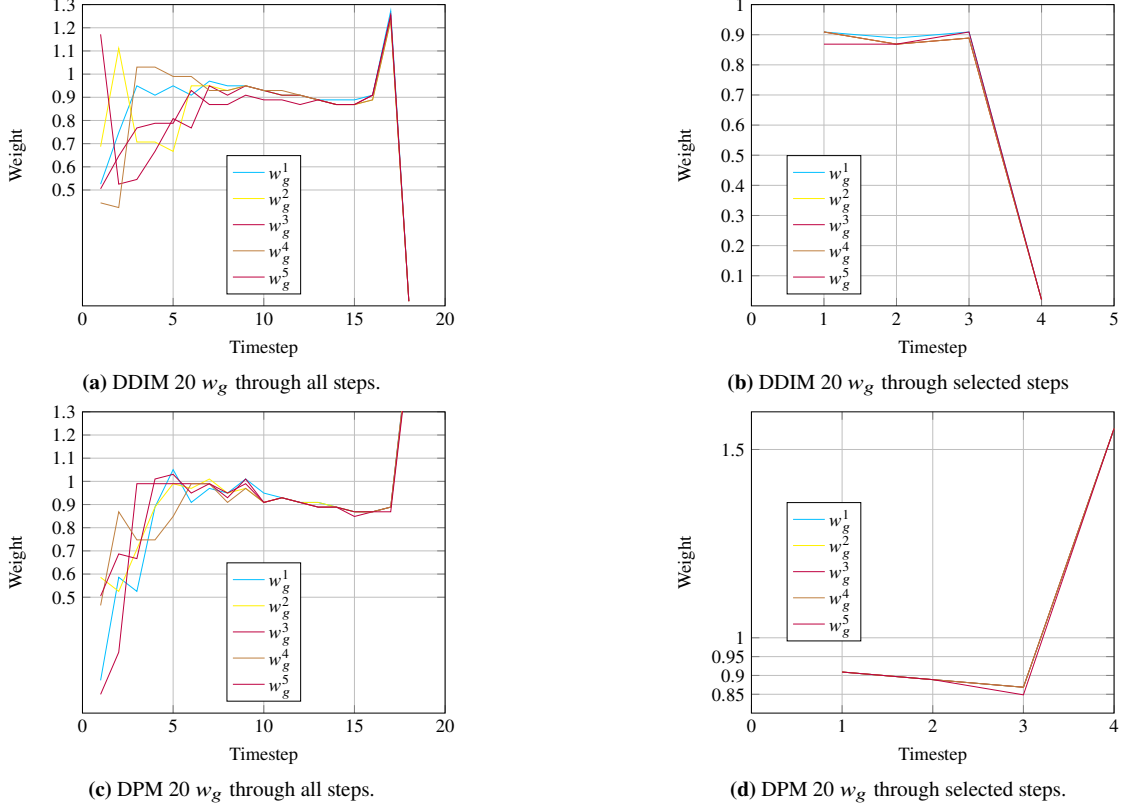


**Figure 6.** Quantitative results of the variation of  $w_g$ . We present our results on DDIM and DPM-Solver++ in 20 steps, with 5 different prompts and latents. Fig. 6a and Fig. 6c demonstrate the original results without acceleration, where  $w_g$  achieves convergence after about 12 steps. Fig. 6b and Fig. 6d show the results within the acceleration interval [12, 20], where different weights are almost the same, indicating strong feature of convergence.

- We select the acceleration condition as  $t \bmod r = r - 1$  and  $t > 4$ , where the period parameter  $r$  is set as  $r = 2$ .
- **Figure 2**
  - (a) The base model is Stable Diffusion v2 [36], and the baseline is DeepCache [26] with 50 steps where  $N = 2$ . We select the acceleration condition as  $t \bmod r = r - 3$  and  $t > 12$ , where the period parameter  $r$  is set as  $r = 3$  only in experiments about DeepCache.
  - (b) The baseline model is Anime-diff [4] model, and the Distillation model is Anime-diff-lightning [20] with 4 steps under the scheduler EDM [8]. We select the acceleration condition as  $t \bmod r = r - 1$  and  $t > 2$ , where the period parameter  $r$  is set as  $r = 2$ .
- **Figure 3**
  - (a) The base model is Stable Diffusion v2, and the corresponding scheduler is DDIM. The result is obtained at 40 steps.
  - (b) We select the acceleration condition as  $t \bmod r = r - 1$  and  $t > 12$  based on the original setting, where the period parameter  $r$  is set as  $r = 2$ .
  - (c) The base model is Stable Diffusion v2, and the

corresponding scheduler is DDIM. The weight values are obtained at 40 steps. Note that the acceleration condition here is ( $t > 1$ ), and the approximated value is not assigned to  $x$  to prevent accumulated errors from deviating the results from the original process.

- **Figure 4**
  - The base model is Stable Diffusion v2, and the corresponding scheduler is DDIM. The result is obtained at 40 steps. We select the acceleration condition as  $t \bmod r = r - 1$  and  $t > 12$  based on the original setting, where the period parameter  $r$  is set as  $r = 2$ . We give trials to a series of bias from 0.0125 to 0.05.
- **Figure 5**
  - The detailed acceleration settings are available in Tab. 6.

## C. Experimental Details

In this section, we give a further insight into relevant details of the experiments mentioned in the paper, including the settings of acceleration intervals, the optional  $w_g$  algorithm.

### C.1. Acceleration Interval

As our method mentioned, we select certain consecutive timesteps as the acceleration interval if the angles formed between their transition operators are less than a threshold  $\tau$ . Typically, we prefer to set  $\tau = 0.1$ . However, the threshold and specific acceleration interval may vary slightly by manual adjustment according to the actual angle plot, in case of a few abnormal angle data samples.

After choosing the acceleration interval, we need to set the period of acceleration, which is defined as the parameter  $r$  in the paper. In most cases, the acceleration is applied at timestep  $\mathbf{x}_t$  within the acceleration interval if  $t \bmod r = r-1$ . Generally,  $r = 2$  is applicable for almost all the cases without any other modification manually, which demonstrates the versatility of our method. The acceleration condition may be adjusted if further improvements in generation quality are required.

#### Text-to-image Synthesis Task

Tab. 6 presents the detailed results of all the experiments we conduct on Stable Diffusion v2 and v3.5-mid in the text-to-image synthesis task, with acceleration settings attached. And Tab. 7 and Tab. 8 show the acceleration settings of each group. Notably,  $r = 2$  is across all these experiments, except for the case that  $r = 3$  in the experiment with DeepCache in Tab. 7.

#### Text-to-video Synthesis Task

We evaluate video quality from two perspectives: Frame Consistency and Textual Faithfulness. For Frame Consistency, we compute CLIP image embeddings for every frame of the output video and report the average cosine similarity among all frame pairs. For Textual Faithfulness, we compute the average ImageReward score between each output video frame and its corresponding edited prompt. From the results, we achieve a  $1.54\times$  speedup with almost no impact on video generation quality.

Tab. 9 gives a specific view of the acceleration settings for the experiments we conduct on video models in the text-to-video synthesis task. In addition, Tab. 10 presents the acceleration settings in distillation as well. All the experiments keep consistent in  $r = 2$ .

#### Ablation Study

The acceleration framework in the ablation experiment with "Skipping Steps" strategy is shown in Tab. 11. In addition, we conduct further ablation studies on Align Your Steps and present results together with acceleration settings in Tab. 12.

### C.2. Optional $w_g$ Algorithm

The optional  $w_g$  algorithm is designed to further minimize the difference between the  $w_g$  we obtain and the optimal one, since in each iteration we just compute an approximate solution. However, most of the experiments demonstrate

that even without the optional  $w_g$  algorithm our method can achieve promising effects on various models and schedulers, with little bias from the original process. Therefore, we apply the optional algorithm only to DDIM.

## D. Visual Results from Selected Experiments

To provide a more intuitive presentation of our experimental results, we have selected representative images from our experiments for visualization. For video experiments, only the first frame is extracted for comparison. The experimental settings correspond to the displayed images as follows.

- **Fig. 7** Results obtained using DDIM sampling on Stable Diffusion v2.
- **Fig. 8** Results obtained using EDM sampling on Stable Diffusion v3.5.
- **Fig. 9** Results obtained using DPMsolver++ sampling on Stable Diffusion v3.5.
- **Fig. 10** Based on the DeepCache model, the results obtained using DDIM sampling on Stable Diffusion v2.
- **Fig. 11** Based on the Align Your Steps method, we obtained sampling results using DPM-Solver++ on Stable Diffusion v1.5.
- **Fig. 12** Results obtained using DDIM sampling on CogVideoX-2B.
- **Fig. 13** Using EDM sampling on the anime-diff model based on epiCRealism.
- **Fig. 14** Using EDM sampling on the anime-diff model based on realistic-vision.
- **Fig. 15** Using EDM sampling on the anime-diff-lightning model based on epiCRealism.
- **Fig. 16** Using EDM sampling on the anime-diff-lightning model based on realistic-vision.



Metric	Model	Scheduler	Original		LTC-ACCEL		Acceleration Condition	Speedup
			Inference Step	Metric Value	Inference Step	Metric Value		
ImageReward	SD v2	DDIM	10	-0.5070	6	0.0261	$t \bmod r = r - 1$ and $t > 2$	1.67×
ImageReward	SD v2	DDIM	20	0.3185	12	0.3117	$t \bmod r = r - 1$ and $t > 4$	1.67×
ImageReward	SD v2	DDIM	30	0.3578	20	0.3541	$t \bmod r = r - 1$ and $t > 10$	1.50×
ImageReward	SD v2	DDIM	40	0.3967	26	0.4009	$t \bmod r = r - 1$ and $t > 12$	1.54×
ImageReward	SD v2	DDIM	50	0.4209	30	0.4183	$t \bmod r = r - 1$ and $t > 10$	1.67×
ImageReward	SD v2	DDIM	100	0.4266	60	0.4316	$t \bmod r = r - 1$ and $t > 20$	1.67×
ImageReward	SD v3.5	DPM-Solver++	12	0.4795	8	0.4796	$t \bmod r = r - 1$ and $t > 4$	1.50×
ImageReward	SD v3.5	DPM-Solver++	24	0.9249	16	0.9287	$t \bmod r = r - 1$ and $t > 8$	1.50×
ImageReward	SD v3.5	DPM-Solver++	36	1.0254	24	1.0313	$t \bmod r = r - 1$ and $t > 12$	1.50×
ImageReward	SD v3.5	DPM-Solver++	48	1.0990	32	1.1016	$t \bmod r = r - 1$ and $t > 16$	1.50×
ImageReward	SD v3.5	DPM-Solver++	60	1.0755	40	1.0785	$t \bmod r = r - 1$ and $t > 20$	1.50×
ImageReward	SD v3.5	EDM	20	0.9351	13	0.9089	$t \bmod r = r - 1$ and $t > 6$	1.53×
ImageReward	SD v3.5	EDM	30	1.0166	19	1.0040	$t \bmod r = r - 1$ and $t > 8$	1.58×
ImageReward	SD v3.5	EDM	40	1.0578	26	1.0497	$t \bmod r = r - 1$ and $11 \leq t \leq 37$	1.54×
ImageReward	SD v3.5	EDM	50	1.0725	30	1.0623	$t \bmod r = r - 1$ and $t > 10$	1.67×
ImageReward	SD v3.5	EDM	60	1.0766	39	1.0691	$t \bmod r = r - 1$ and $15 \leq t \leq 55$	1.54×
PickScore	SD v2	DDIM	10	20.08	6	21.09	$t \bmod r = r - 1$ and $t > 2$	1.67×
PickScore	SD v2	DDIM	20	21.53	12	21.52	$t \bmod r = r - 1$ and $t > 4$	1.67×
PickScore	SD v2	DDIM	30	21.60	20	21.59	$t \bmod r = r - 1$ and $t > 10$	1.50×
PickScore	SD v2	DDIM	40	21.66	26	21.65	$t \bmod r = r - 1$ and $t > 12$	1.54×
PickScore	SD v2	DDIM	50	21.69	30	21.69	$t \bmod r = r - 1$ and $t > 10$	1.67×
PickScore	SD v2	DDIM	100	21.73	60	21.73	$t \bmod r = r - 1$ and $t > 20$	1.67×
PickScore	SD v3.5	DPM-Solver++	12	21.23	8	21.21	$t \bmod r = r - 1$ and $t > 4$	1.50×
PickScore	SD v3.5	DPM-Solver++	24	21.93	16	21.95	$t \bmod r = r - 1$ and $t > 8$	1.50×
PickScore	SD v3.5	DPM-Solver++	36	22.19	24	22.21	$t \bmod r = r - 1$ and $t > 12$	1.50×
PickScore	SD v3.5	DPM-Solver++	48	22.26	32	22.28	$t \bmod r = r - 1$ and $t > 16$	1.50×
PickScore	SD v3.5	DPM-Solver++	60	22.33	40	22.35	$t \bmod r = r - 1$ and $t > 20$	1.50×
PickScore	SD v3.5	EDM	20	22.28	13	22.23	$t \bmod r = r - 1$ and $t > 6$	1.53×
PickScore	SD v3.5	EDM	30	22.43	19	22.28	$t \bmod r = r - 1$ and $t > 8$	1.58×
PickScore	SD v3.5	EDM	40	22.51	26	22.49	$t \bmod r = r - 1$ and $11 \leq t \leq 37$	1.54×
PickScore	SD v3.5	EDM	50	22.53	30	22.52	$t \bmod r = r - 1$ and $t > 10$	1.67×
PickScore	SD v3.5	EDM	60	22.53	39	22.52	$t \bmod r = r - 1$ and $15 \leq t \leq 55$	1.54×

**Table 6.** Text-to-image Synthesis on Stable Diffusion.

Model	DeepCache			LTC-ACCEL			Acceleration Condition	Speedup
	Inference Step	Time	Image Reward	Inference Step	Time	Image Reward		
SD v2	10	264	-0.2246	8	208	-0.2739	$t \bmod r = r - 1$ and $t > 4$	1.25×
	20	524	0.2445	16	419	0.2456	$t \bmod r = r - 1$ and $t > 8$	1.25×
	50	1411	0.4039	38	1038	0.4096	$t \bmod r = r - 3$ and $t > 12$	1.41×
	100	3014	0.4242	75	2171	0.4246	$t \bmod r = r - 3$ and $24 < t \leq 90$	1.38×

**Table 7.** Quantitative results of text-to-image, combining our method with Deepcache, where the parameter  $N$  mentioned in DeepCache remains  $N = 2$ .

Model	Scheduler	Original		Ays		LTC-ACCEL		Acceleration Condition	Speedup
		Inference Step	Image Reward	Inference Step	Image Reward	Inference Step	Image Reward		
SD v1.5	DPM-Solver++	10	0.1111	10	0.1332	8	0.1309	$t \bmod r = r - 1$ and $t > 6$	1.25×

**Table 8.** Quantitative results of text-to-image, combining our method with Align Your Steps.

Model	Inference Step	Original		Inference Step	LTC-ACCEL		Acceleration Condition	Speedup
		Image Reward	Frame Consistency		Image Reward	Frame Consistency		
epiCRealism	10	0.2439	0.9713	7	0.2426	0.9700	$t \bmod r = r - 1$ and $t > 4$	1.43×
epiCRealism	20	0.3050	0.9729	13	0.2939	0.9732	$t \bmod r = r - 1$ and $t > 6$	1.54×
epiCRealism	30	0.3662	0.9676	19	0.3465	0.9681	$t \bmod r = r - 1$ and $t > 8$	1.58×
realistic-vision	10	0.1142	0.9636	7	0.1135	0.9633	$t \bmod r = r - 1$ and $t > 4$	1.43×
realistic-vision	20	0.2646	0.9676	13	0.2683	0.9672	$t \bmod r = r - 1$ and $t > 6$	1.54×
realistic-vision	30	0.4046	0.9655	19	0.3913	0.9669	$t \bmod r = r - 1$ and $t > 8$	1.58×
CogVideoX-2B	20	-0.1441	0.9442	14	-0.1673	0.9361	$t \bmod r = r - 1$ and $t > 8$	1.43×
CogVideoX-2B	30	0.2302	0.9464	19	0.2320	0.9435	$t \bmod r = r - 1$ and $t > 8$	1.58×
CogVideoX-2B	40	0.3918	0.9514	26	0.3775	0.9511	$t \bmod r = r - 1$ and $t > 12$	1.54×

**Table 9.** Quantitative results of text-to-video. We present our results on Anime-diff, and CogVideoX by measuring the Textual Faithfulness and Frame Consistency using 100 prompt-video pairs.

Model	Inference Step	Original		Inference Step	Original		Inference Step	LTC-ACCEL		Acceleration Condition	Speedup
		Image Reward	Frame Consistency		Image Reward	Frame Consistency		Image Reward	Frame Consistency		
epiCRealism	4	0.3662	0.9685	3	0.2913	0.9673	3	0.3550	0.9645	$t \bmod r = r - 1$ and $t > 2$	1.33×
epiCRealism	8	0.3371	0.9697	5	0.2978	0.9690	5	0.3493	0.9654	$t \bmod r = r - 1$ and $t > 2$	1.60×
realistic-vision	4	0.2412	0.9639	3	0.1249	0.9641	3	0.2156	0.9618	$t \bmod r = r - 1$ and $t > 2$	1.33×
realistic-vision	8	0.2469	0.9623	5	-0.0095	0.9635	5	0.2237	0.9598	$t \bmod r = r - 1$ and $t > 2$	1.60×

**Table 10.** Quantitative results of text-to-video, combining our method with anime-diff-lightning (the distilled version of anime-diff).

Model	Scheduler	Skipping Steps		LTC-ACCEL		Acceleration Condition
		Steps	ImageReward↑	Steps	ImageReward↑	
SD v2	DDIM	7	0.0537	7	0.1472	$t \bmod r = r - 1$ and $t > 4$
	DDIM	10	0.2003	10	0.2442	$t \bmod r = r - 1$ and $t > 6$
	DDIM	13	0.2812	13	0.3129	$t \bmod r = r - 1$ and $t > 6$
SD v2	EDM	7	0.0158	7	0.2018	$t \bmod r = r - 1$ and $t > 4$
	EDM	10	0.2003	10	0.3171	$t \bmod r = r - 1$ and $t > 6$
	EDM	13	0.2582	13	0.3335	$t \bmod r = r - 1$ and $t > 6$

**Table 11.** Ablation study comparing LTC-ACCEL with the Skipping Steps method, where Skipping Steps maintains the same acceleration positions as ours.  $r = 2$  is consistent in the ablation study.

Model	Scheduler	Ays + Skip-steps		Ays + LTC-ACCEL		Acceleration Condition
		Inference Step	Image Reward	Inference Step	Image Reward	
SD v1.5	DPM-Solver++	8	0.0820	8	0.1309	$t \bmod r = r - 1$ and $t > 6$

**Table 12.** Ablation study comparing our method with Align Your Steps (Ays), where Ays maintains the same acceleration positions as ours.  $r = 2$  is consistent in the ablation study.

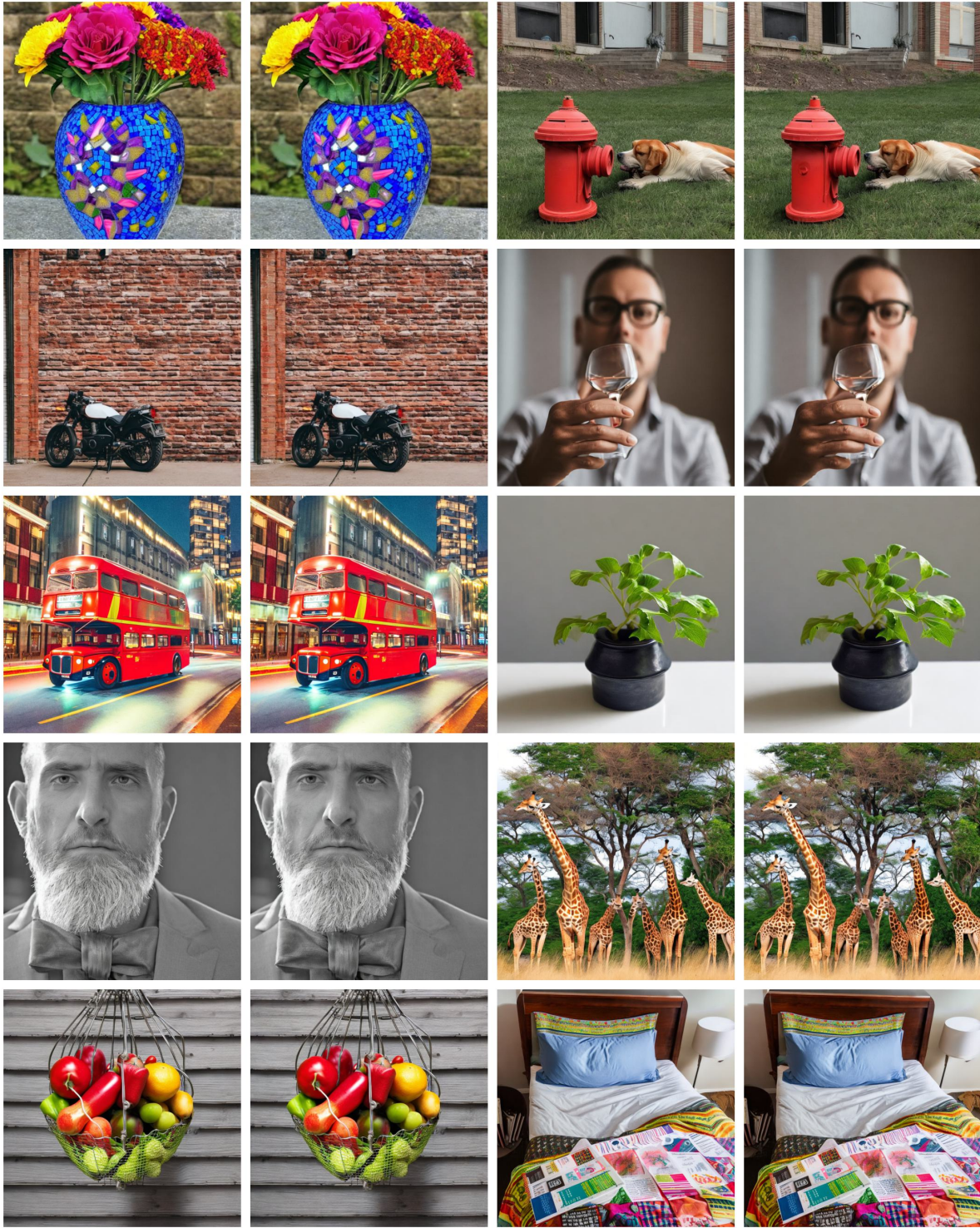


**Figure 7.** Results obtained using DDIM sampling on Stable Diffusion v2 are shown. In each row, the first and third images correspond to the 50-step outputs from the original process, while the remaining two images display the LTC-ACCEL results achieved in just 30 steps.



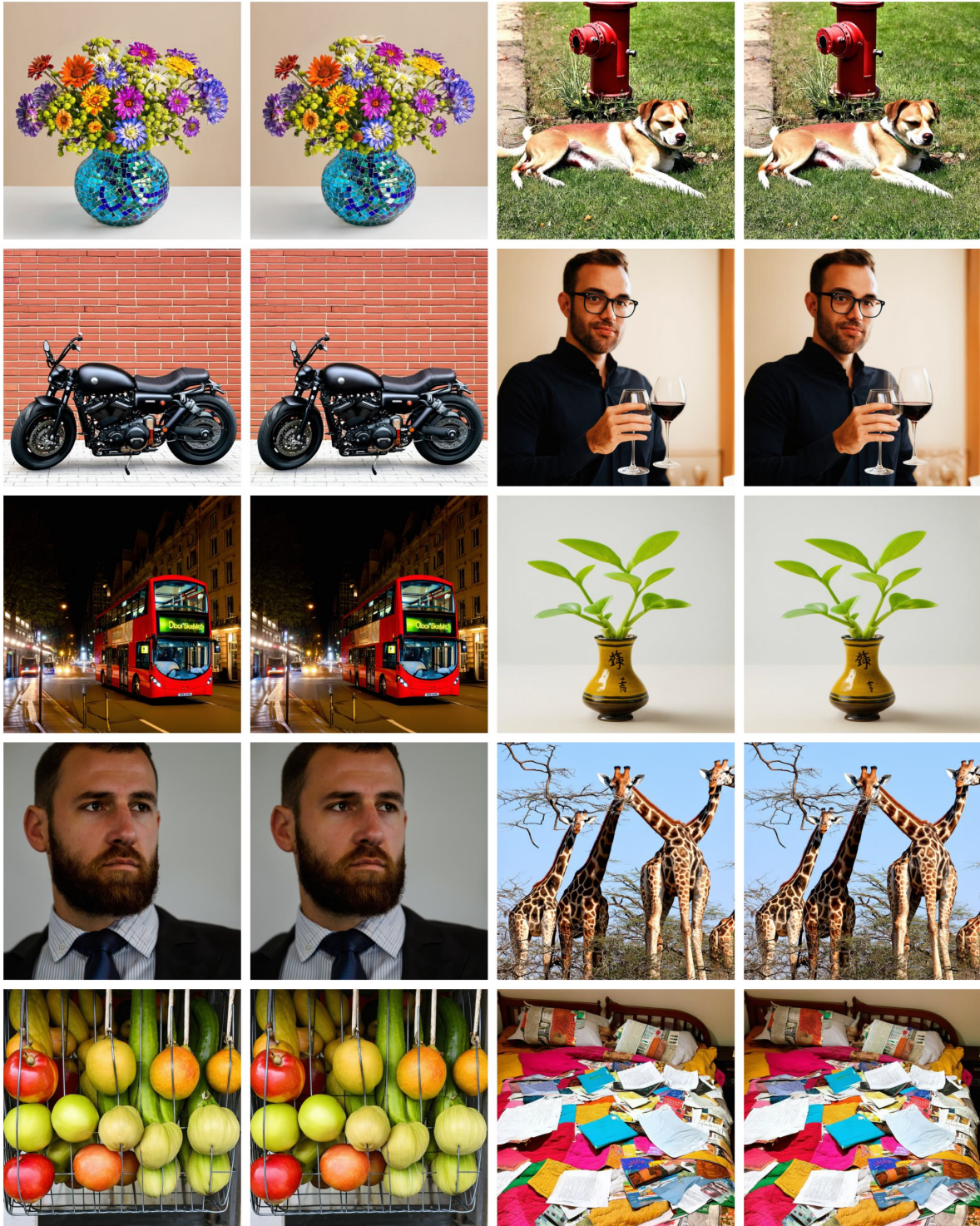


**Figure 8.** Results obtained using EDM sampling on Stable Diffusion v3.5 are shown. In each row, the first and third images correspond to the 60-step outputs from the original process, while the remaining two images display the LTC-ACCEL results achieved in just 39 steps.



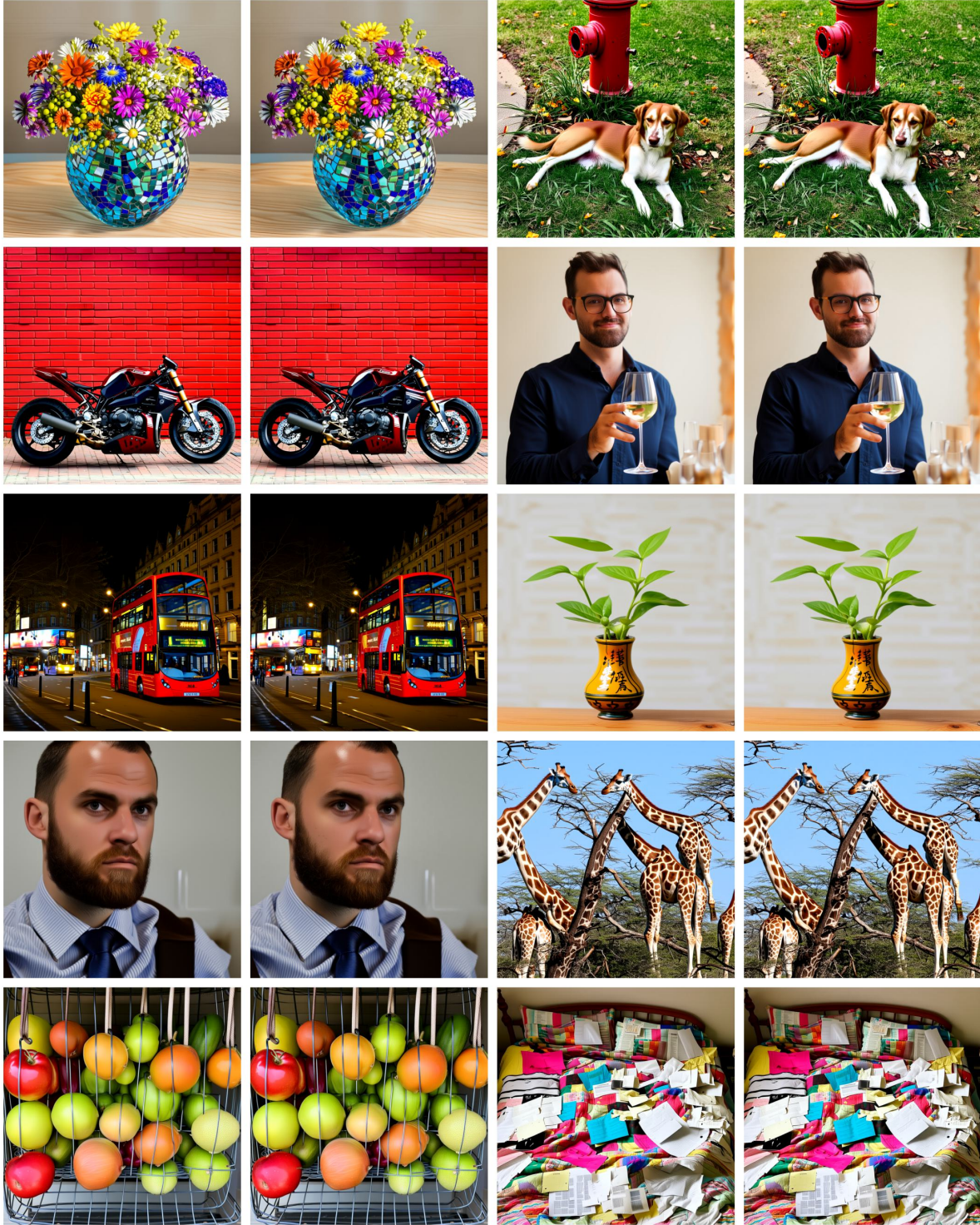


**Figure 9.** Results obtained using DPMsolver++ sampling on Stable Diffusion v3.5 are shown. In each row, the first and third images correspond to the 60-step outputs from the original process, while the remaining two images display the LTC-ACCEL results achieved in 40 steps.



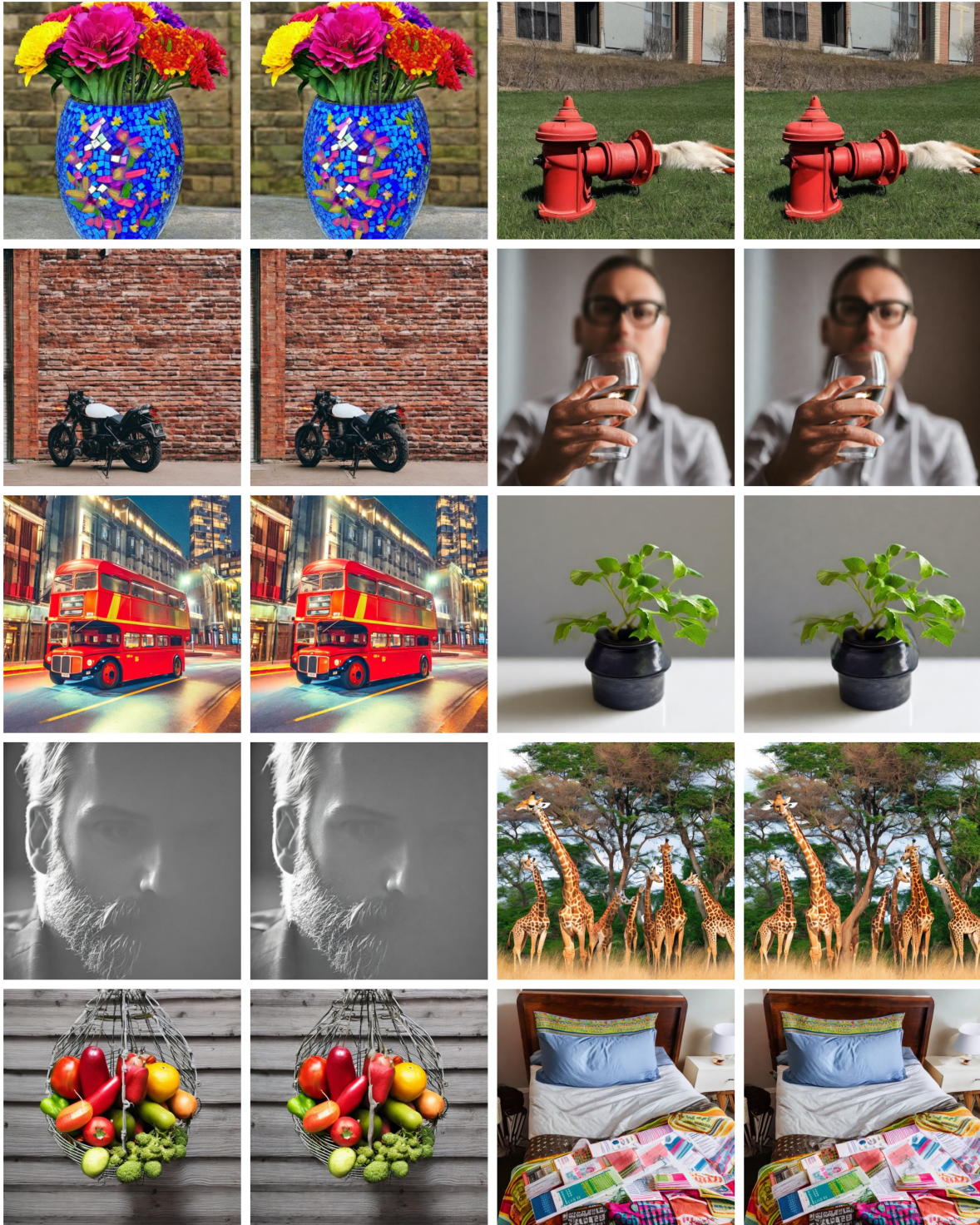


**Figure 10.** Based on the DeepCache model, the results obtained using DDIM sampling on Stable Diffusion v2 are presented. In each row, the first and third images depict the DeepCache results after 50 iterations, while the remaining two images display the outputs from LTC-ACCEL combined with DeepCache after 38 iterations.



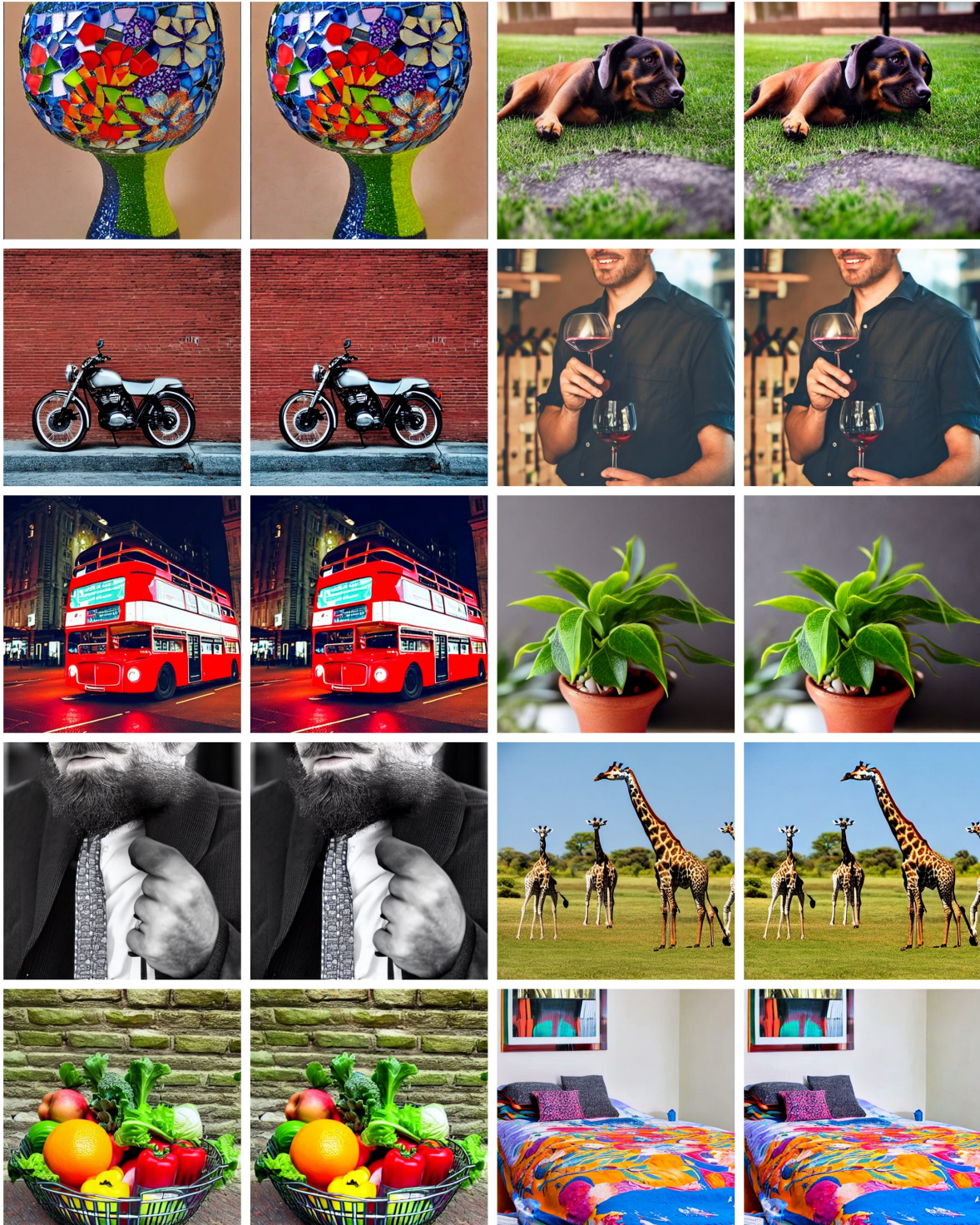


**Figure 11.** Based on the Align Your Steps method, we obtained sampling results using DPM-Solver++ on Stable Diffusion v1.5. In each row, the first and third images represent the outputs after 10 iterations using only the “Align Your Steps” approach, while the second and fourth images show the results achieved by combining LTC-ACCEL with align your step for 8 iterations.



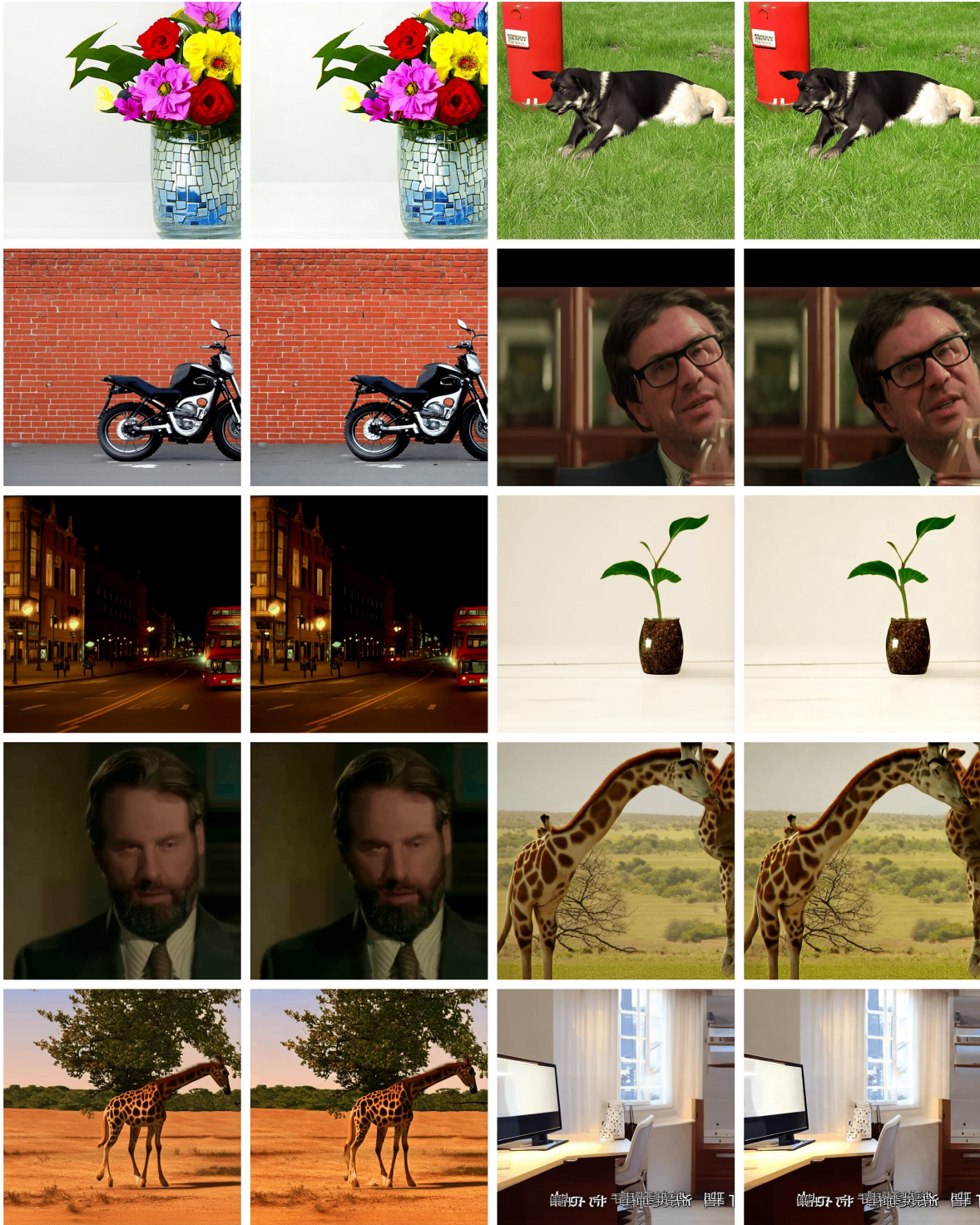


**Figure 12.** Results obtained using DDIM sampling on CogVideoX-2B, with only the first frame of each video selected. In each row, the first and third images represent the outputs after 40 iterations of the original process, while the remaining two images display the LTC-ACCEL results achieved in 26 iterations.



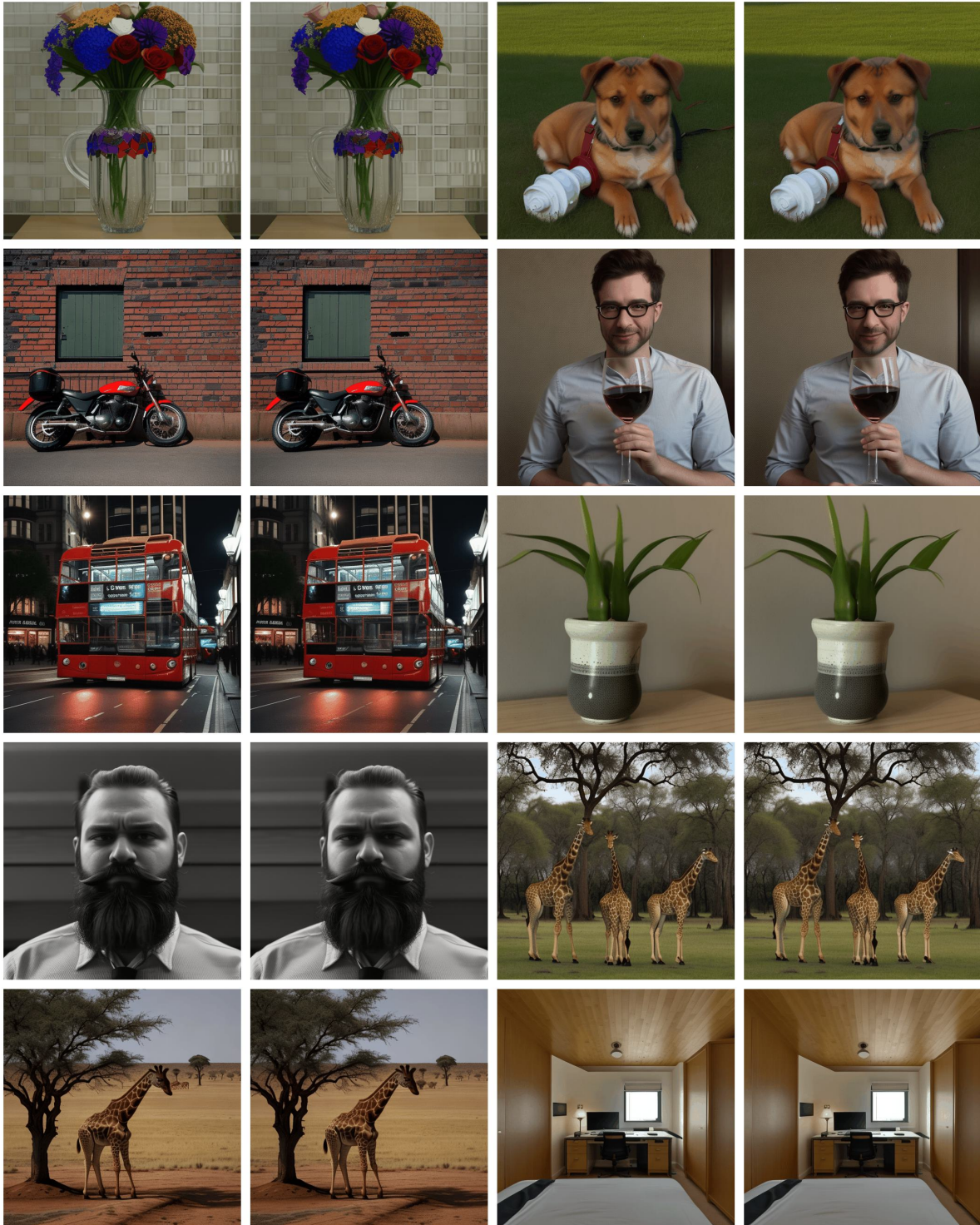


**Figure 13.** Using EDM sampling on the anime-diff model based on epiCRealism, we obtained results where only the first frame of each video was selected. In each row, the first and third images correspond to the outputs after 30 iterations of the original process, while the remaining two images show the LTC-ACCEL results achieved in 19 iterations.



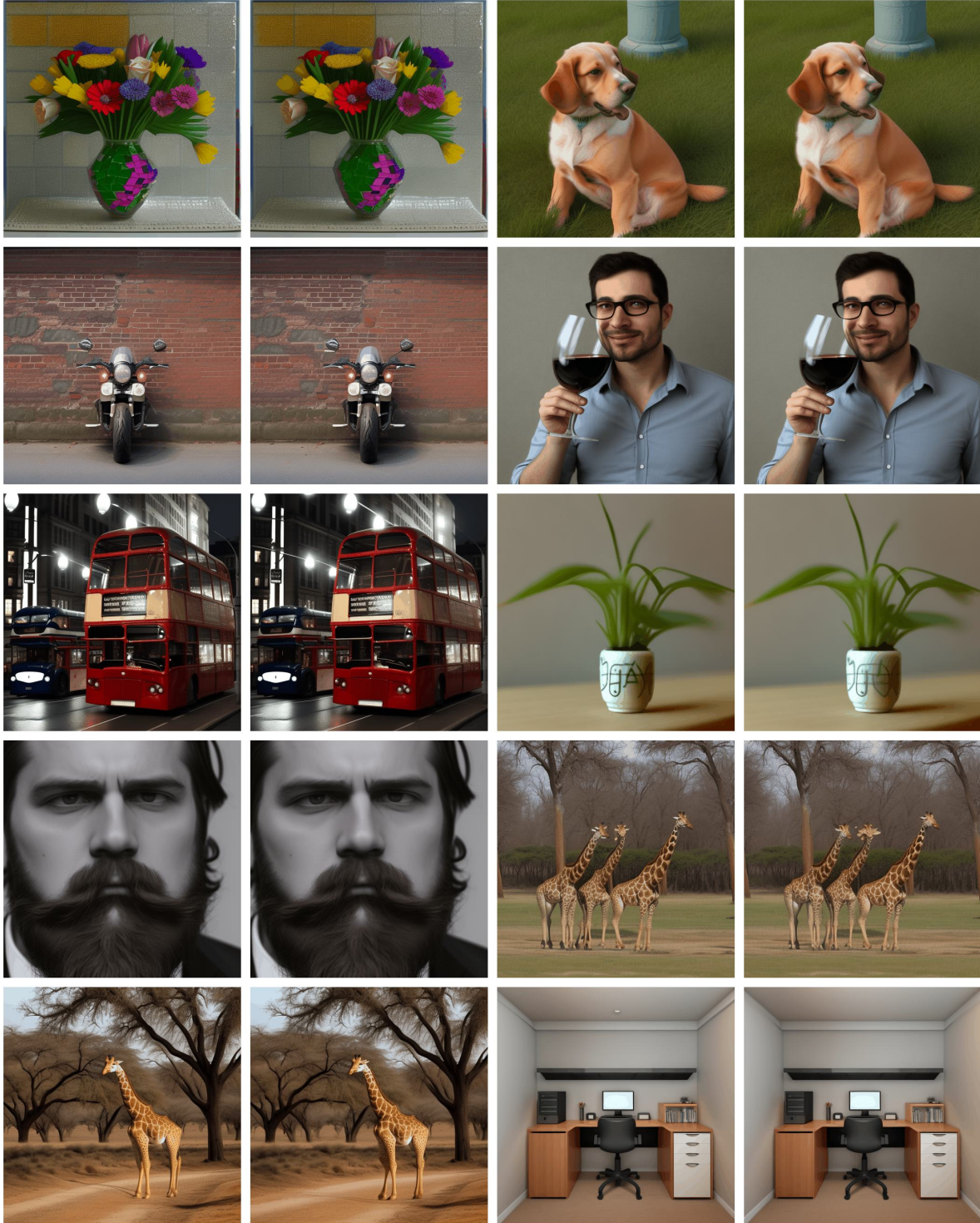


**Figure 14.** Using EDM sampling on the anime-diff model based on realistic-vision, we obtained results where only the first frame of each video was selected. In each row, the first and third images correspond to the outputs after 30 iterations of the original process, while the remaining two images show the LTC-ACCEL results achieved in 19 iterations.



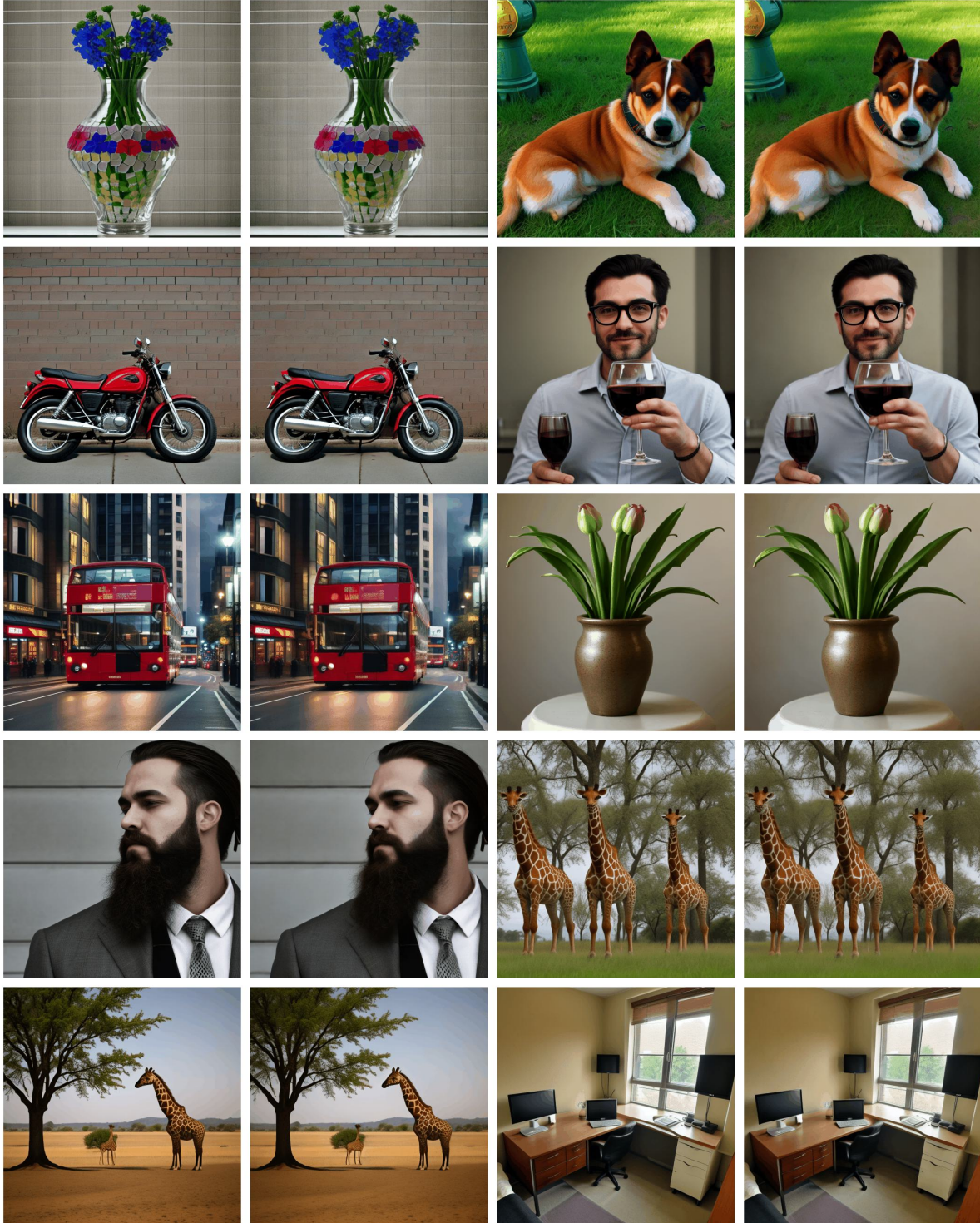


**Figure 15.** Using EDM sampling on the anime-diff-lightning model based on epiCRealism, we obtained results where only the first frame of each video was selected. In each row, the first and third images correspond to the outputs after 4 iterations of the original process, while the remaining two images show the LTC-ACCEL results achieved in 3 iterations.



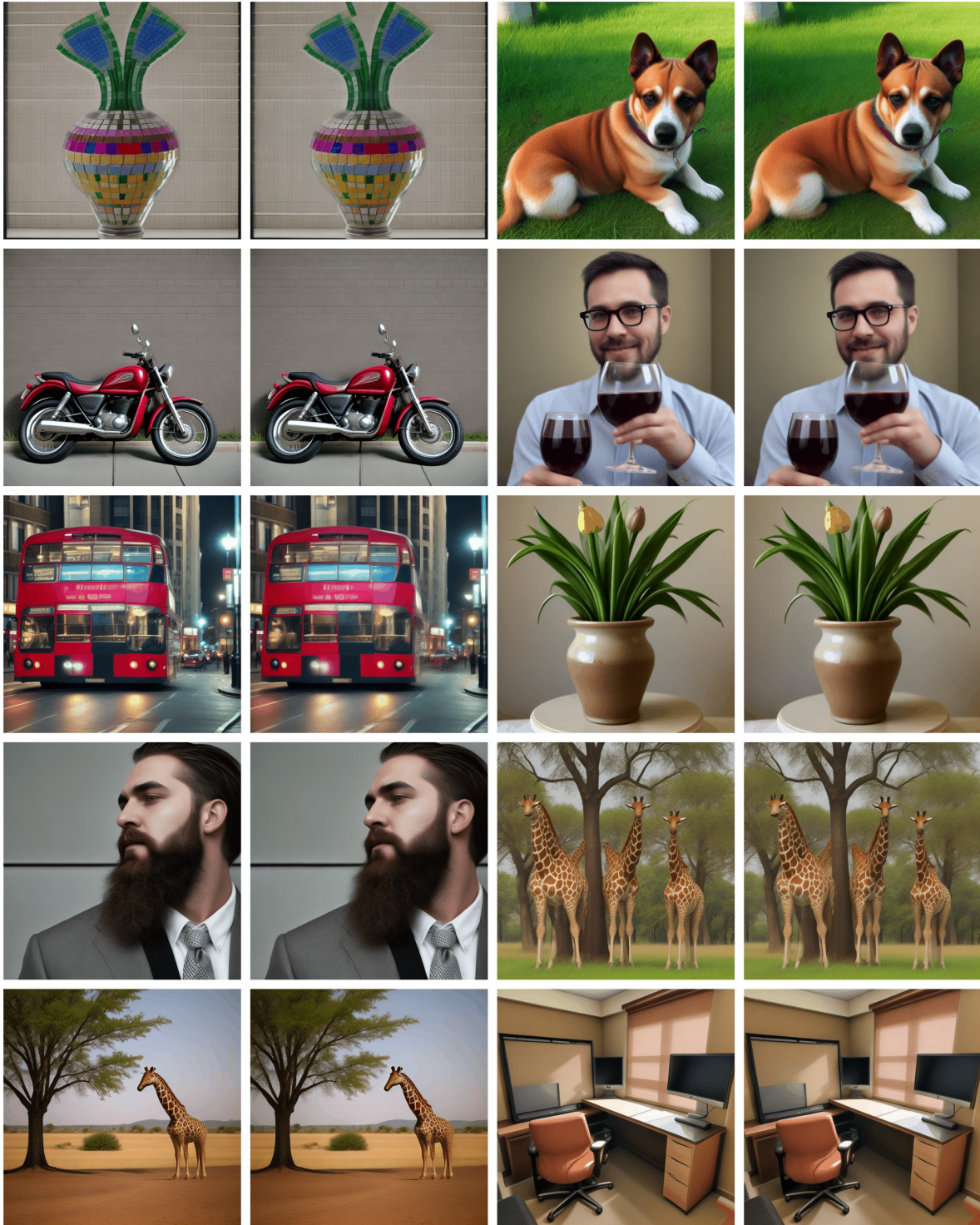


**Figure 16.** Using EDM sampling on the anime-diff-lightning model based on realistic-vision, we obtained results where only the first frame of each video was selected. In each row, the first and third images correspond to the outputs after 4 iterations of the original process, while the remaining two images show the LTC-ACCEL results achieved in 3 iterations.